UNIVERSITÀ DEGLI STUDI DELLA TUSCIA DI VITERBO

DIPARTIMENTO DI ECOLOGIA E BIOLOGIA

Corso di Dottorato di Ricerca in

GENETICA E BIOLOGIA CELLULARE XXVII Ciclo

TITOLO TESI DI DOTTORATO DI RICERCA

Animals model to visualise proliferation events in living animals via noninvasive bioluminescence imaging technology.

(s.s.d. BIO/11)

Tesi di dottorato di:

Dott.ssa Luisa de Latouliére

Firma Luisa de Latouliére

Coordinatore del corso	**Tutore**
Prof. Giorgio Prantera	Dott.ssa Giulia Piaggio
Firma ……..	Firma ……

Data della discussione 06/05/2016

Contents

1. TITLE

Animals model to visualise proliferation events in living animals via noninvasive bioluminescence imaging technology.

2. ABSTRACT

Mouse and Zebrafish models represent a critical step to improve treatments of malignant disease, as an intermediate method of experimentation between cell culture based assays and human clinical trials. Most of the cellular pathways are highly conserved between human, mouse and Zebrafish, thus rendering zebrafish model very attractive. Recently we have generated a transgenic reporter mouse, called MITO-Luc, in which the luciferase reporter gene are placed under the control of cyclinB2 minimal promoter containing three CCAAT boxes tightly regulated by the transcription factor NF-Y. In these mice, BioLuminescence Imaging (BLI) of NF-Y activity visualizes areas of physiological cell proliferation and regeneration during response to injury.

During my PhD thesis I have developed and characterized two pancreatic cancer disease models, MITO-Luc-KC and MITO-Luc-KPC mice, obtained through intercross with our MITO-Luc mouse model with models for pancreatic ductal adenocarcinoma (PDAC), LSL-Kras$^{G12D/+}$;Pdx-1-Cre (KC) and LSL-Kras$^{G12D/+}$;LSL-Trp53$^{R172H/+}$;Pdx-1-Cre (KPC) mice. In these models Cre-recombinase regulated by a pancreas-specific promoter activates the expression of oncogenic Kras alone or in combination with a mutant p53, respectively. In these mice we have had the opportunity to follow PDAC evolution in the living animal in a time frame process.

Parallel to the above described mouse models, during my PhD thesis I have also generated a zebrafish model which allows us to visualize through BLI any proliferation events in the context of the entire alive animal during development and adult life. In this transgenic line, luciferase and GFP reporter genes are placed under control of the same proliferation dependent promoter that we have already employed in mice. In these zebrafish model we have observed an ubiquitous GFP and bioluminescence signal in early living embryos while they become tissue specific at 33hpf (hour post fertilization embryos, in juveniles and adult zebrafish animals. To understand if the luciferase activity does occur in proliferating cells we have tested the effect of well-known antiproliferative drugs and treatments, and we have observed that the luciferase activity was inhibited by 5FU and X-Ray on zebrafish embryos. Finally we have analyzed the bioluminescence signal in alive adult Zebrafish after fin clip. We have observed an early systemic proliferation signal in the whole animal, and later a signal focused on the tail regenerating. The use of BLI on our zebrafish model as read out for proliferation events would speed up in the future the evaluation of anti- or pro-proliferative drug candidates.

3. PREFACE

3.1. Bioluminescence Imaging

In vivo optical imaging represents an interesting current and future new approach to molecular imaging. It allows imaging of internally generated light linked to specific biological functions, by both physiological and pathological processes in living small animals. This noninvasive technique, allows quantification in the same animal of spatial and temporal progression of the interest process and identification of animal-to-animal variations (Signore *et al*., 2010).

One strategy to use optical imaging in living animals is the use of luciferase reporter genes as internal sources of light. This strategy, called BioLuminescence Imaging (BLI), enables real-time noninvasive imaging of several biological processes ranging from infections to gene expression in living organisms. The sensitivity of detecting internal light generated by luciferase in an intact animal is dependent upon many parameters. One crucial issue is the depth of the luciferase-labeled cells (host or pathogen) within the body. In other words, the distance that the photons must travel through tissues to exit the animal's body surface strongly influences the sensitivity of the system. The light emitted by luciferase is able to penetrate tissue depths of the order of several millimeters to centimeters; however, photon intensity decreases 10-fold for each centimeter of tissue depth (Sato *et al*., 2004). In the context of mouse models, experimental attenuations due to skin effects of a factor of 2-10 have been demonstrated. It seems that about 12% of the in situ luminescence appeared available for noninvasive imaging due to scattering and absorption in subcutaneous tissue and skin (Sharma *et al*., 2010; O'Neill *et al*., 2010). In addition to attenuation of light by overlying tissues, BLI is decreased by pigmentation of fur. Shaving mice with electric clippers or removing fur with a depilatory agent can minimize this problem. Alternatively, mice can be bred into an albino background, or mice without skin pigmentation can be employed (Rocchetta *et al*., 2001; Luker *et al*., 2005). In the context of zebrafish models, due to the small size of fishes that reaches 4 cm in length and 0,5 cm of thickness, difficulties about tissue penetration are slight, owing to the shorter distance through which the emitted light has to travel to reach body surface. Recently Chen's group has found that luciferase activity in adult Zebrafish can be reproducibly monitored in tissues of freely swimming animals in a noninvasive manner. Although melanin absorbs light, the photons emitted from internal fonts do not show signal attenuation by the melanophores longitudinal stripes (Chen *et al*., 2013).

Overall, the limit of detection will diverge between different models due to the varying strength of the promoter used to drive luciferase expression. The sensitivity of detection devices used is also an important variable that influences the sensitivity of this noninvasive optical imaging

technique. To acquire images of small animals expressing luciferase, instruments have been developed equipped with cooled Charge-Coupled Device (CCD) cameras (Fig.1A). Supercooling the CCD camera reduces the thermal noise of the systems, increasing signal-to-noise ratio and preserving spectral sensitivity. Indeed, these cameras are sensitive to light across the entire visible spectrum and into the near-infrared. CCD cameras used for *in vivo* imaging of living animals are mounted inside a light tight box in which the anesthetized animals are placed and imaged. Typically, the camera is accompanied with computer software for image data acquisition and analysis. The software converts electron signals into a two-dimensional image, quantifies the intensity of the emitted light (number of emitted photons striking the detectors), and converts these numerical values into a pseudocolor graphic. The actual data are measured in photons, but the pseudocolor graphic enables rapid visual interpretation. The data are quantified by Region-Of-Interest (ROI) analysis, measuring photon flux from bioluminescence. For quantification purposes, it is important to know that there is a variable attenuation of light by different organs and tissues.

Generally, BLI is a simple and rapid imaging technique as compared to others for preclinical studies, with accessible costs, making this technique relatively inexpensive and available for most research laboratories. It is important to keep in mind that all conventional devices produce 2D images. The optical signals coming from a given ROI may therefore represent the summation of overlapping anatomic structures. Moreover, because the spatial resolution of BLI is 2-3 mm, the technique cannot differentiate between sources of light emanating from anatomical sites that are close together (Signore *et al*., 2010). Recently, a device has been developed that allows a 3D diffuse luminescence tomography (DLIT) (Thompson *et al*., 2013). DLIT is a method that takes into account the scattering and absorption of light in tissue and provides an estimate of the 3D location and brightness of the light-emitting sources (IVIS 200 Imaging System).

BLI technology has been applied in studies to monitor dissemination and progression of viral and bacterial infections, chronic and acute inflammation, cell transplantation, active proliferation, tumor growth and metastasis, response to therapy, drug discovery, and gene expression (Contag, 2008; Hutchens and Luker, 2007; Doyle *et al*., 2004; Goeman *et al*., 2012; Coleman and McGregor, 2015). BLI detects light produced by the enzymatic reaction of a luciferase enzyme with its substrate in the context of living animals. This enzymatic production of visible light is a naturally occurring phenomenon in many nonmammalian species, and there are a variety of luciferase enzymes coming from different organisms. Many of these have been used to transfect both pathogens and host cells (Luker and Luker, 2008). Bioluminescence is produced from several organisms among which firefly (*Photinus pyralis*) or sea pansy (*Renilla reniliformis*) or can

be acquired from bacterial lux operons (*Photorhabdus luminescens, Xenorhabdus luminescens*) (Hutchens and Luker, 2007).

The most common molecular imaging reporter used in eukaryotic cells is the firefly (*Photinus pyralis*) luciferase, normally a heat-unstable enzyme with a biological half-life of approximately 2h. Heat-stable variants of firefly luciferase have been also produced (Law *et al*., 2006). These mutant enzymes are very promising due to their greater light emission, but they are not yet used routinely. However, the short half-life of the wild type firefly luciferase allows studies of the dynamics of biological processes such as changes in pathogen replication, promoter activation, etc. Mouse animal models do not produce the substrate for the light producing process, the luciferin, and it must be delivered systemically. The substrate (luciferin) distributes throughout the mouse rapidly after intraperitoneal (IP) or intravenous (IV) injection at saturating levels for the luciferase reaction (about 2.5 mg per 25 g in mice) (Ciana *et al*., 2003). Moreover, it has been demonstrated that luciferase passes across blood-tissue barriers including placenta (Lipshutz *et al*., 2001). It can therefore be imaged in any organ. Likewise in mice, in zebrafish models, luciferin can be injected intraperitoneally or simply dissolved in aquarium water, letting the fish swimming (Chen *et al*., 2013). The enzyme oxidizes luciferin in a reaction that requires oxygen and adenosine triphosphate (ATP), emitting light with a broad emission spectrum with a peak at approximately 560 nm (Fig.1B). Studies of photon diffusion through tissues have indicated that as few as one hundred bioluminescent cells could be detectable at subcutaneous tissue sites (O'Neill *et al*., 2010). Light from firefly luciferase peaks 10-12 min after injection of luciferin and decreases slowly over the next 60 min (Ciana *et al*., 2003), providing a broad time window for image acquisition. Typically, imaging begins 8-10 min after injection.

A

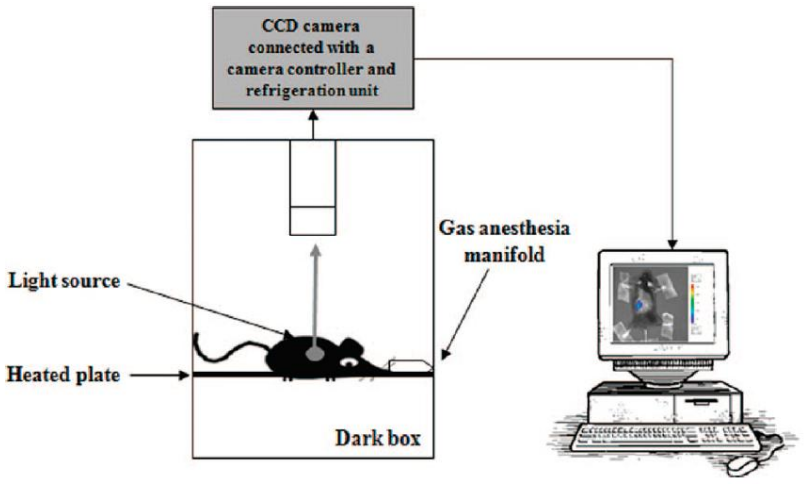

B

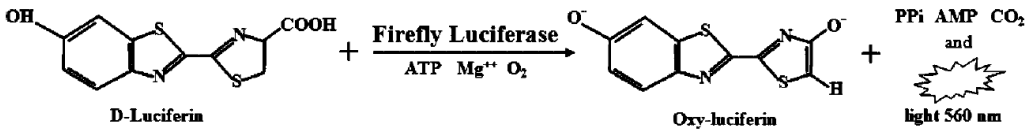

Figure 1. ***Bioluminescence Imaging.*** **(A)** The instrument used for luminescence is based on an ultrasensitive cooled CCD camera connected with a dark box. In the box, there is a shelf heated at 37°C where the animals are located. The CCD camera detects light coming from reporter cells or transgenic animals tagged with luciferase. The images are collected and quantified by advanced dedicated software. (**B)** Bioluminescent reaction catalyzed by firefly luciferase. Firefly luciferase, in the presence of oxygen and in an ATP-dependent manner, catalyzes the oxidation of luciferin to oxyluciferin, which yields light at 560 nm.

3.2. Transgenic luciferase-reporter animals models

Several transgenic mouse models have been developed to study inflammation, immune processes, proliferative events and tumor progression in living animals by BLI. These mice are useful tools for tracking various processes *in vivo*, and also for testing the efficacy of therapeutic compounds that target pathogenesis. Although some models could be missed, the following list represents an update of transgenic models generated to now.

To visualize inflammation processes, transgenic mice that express luciferase driven by three NF-kB response elements (NF-kB-luc mice) have been developed to produce an early and sensitive detection marker of autoimmune disease in intact animals. Treating mice with stressors show an increase of the luminescence in a tissue-specific manner (Carlsen *et al*., 2002). By BLI, the authors showed that airway instillation of *P.aeruginosa*, a major cause of nosocomial pneumonia, resulted in NF-kB activation in the lungs (Sadikot *et al*., 2006). Furthermore it has been demonstrated that NF-kB plays a critical role in the early stages of the host immune response toward coliform intramammary infections, both at the local and at the systemic level (Notebaert *et al*., 2008) Finally, NF-kB-luc mice crossed with autoimmune mouse models have provided a useful tool to demonstrate the role of NFkB activation as an early *in vivo* marker for detection of autoimmune disease (Zangani *et al*., 2009). A transgenic mouse (iNos-luc) has been developed, providing a valuable tool for studying processes in which the inducible NO synthase gene (iNOS) is induced such as septic shock, contact hypersensitivity, rheumatoid arthritis, gastrointestinal disorders, and myocardial ischemia and for screening anti-inflammatory compounds in living animals (Zhang *et al*., 2003). Acute phase serum amyloid A proteins (A-SAAs) are multifunctional apolipoproteins produced in large amounts during the acute phase of inflammation and during the development of chronic inflammatory diseases. A SAA1 promoter-driven luciferase expression transgenic mouse

(Saa1-luc) has been developed. Using these Saa1-luc transgenic mice, a SAA induction in liver and other organs by many inflammatory agents has been shown (Zhang *et al*., 2005). A model for noninvasive imaging of autoimmune encephalomyelitis has been developed using a reporter mouse in which the injury-responsive glial fibrillary acidic protein (GFAP) promoter is fused to luciferase (GFAP-luc mice). In these mice, bioluminescence from the brain and spinal cord correlates strongly with the severity of acute autoimmune encephalomyelitis (Luo *et al*., 2008). An ALS-(GFAP-luciferase/SOD (G93A) reporter mouse in which upregulation of glial fibrillary acidic protein (GFAP) has been generated to further investigate the involvement of glial cells (astrocytes and Schwann cells) in the pathogenesis of Amyotrophic lateral sclerosis (ALS) is a late-onset neurological disease characterized by progressive loss of motor neurons (Keller *et al*., 2009). Two knock-in mice has been generated in which the firefly or the Renilla luciferase reporter enzyme is expressed at the start site of translation of the endogenous cyclooxygenase-2 (Cox-2) gene that plays a role in a variety of normal and pathophysiological conditions including both chronic and acute inflammation, providing tools to analyze Cox-2 expression in inflammation (Ishikawa *et al*., 2006; Kamei *et al*., 2006). A highly sensitive inflammation-monitoring mouse system has been generated using a bacterial artificial chromosome (BAC) clone containing extended flanking sequences of the human interleukin 6 gene (hIL6) locus, in which the luciferase (Luc) reporter gene is integrated (hIL6-BAC-Luc). Systemic inflammation has been monitored in various tissues of the hIL6-BAC-Luc mice using an *in vivo* bioluminescence imaging system. Furthermore when two chronic inflammatory disease models, i.e., a genetic model of atopic dermatitis and a model of experimental autoimmune encephalomyelitis (EAE), were applied to the hIL6-BAC-Luc mice, luciferase bioluminescence was specifically detected in the atopic skin lesion and central nervous system, respectively (Hayashi *et al*., 2015).

To determine the dynamics of estrogen receptor activity and the dependence of estrogen receptor on 17 beta-estradiol *in vivo*, transgenic mouse that expresses a luciferase reporter gene under the control of activated estrogen receptors has been generated. This study has been the pioneer in the field of transgenic luciferase-reporter animals models and, using immature mice before gonadal production of sex hormones as well as ovariectomized adult mice, it highlights, for the first time, the importance of hormone-independent activation of the estrogen receptor (Ciana *et al*., 2003). In the field of hormone receptor activities a transgenic mouse for the detection of PPARs activities has been generated. In this model luciferase expression is under the control of a PPAR-inducible promoter in all target organs, providing an opportunity for the molecular characterization of PPAR activity in patho/physiological conditions (Ciana *et al*., 2007).

To measure tumor growth noninvasively, transgenic mice have been developed that express the luciferase gene under the control of the E2F1 promoter crossed with genetically defined mouse model of human gliomas. The power of this system is that it enables tumor evolution and detection of spontaneous tumors at early stages of development as they evolve within their natural microenvironment. This system can be used to identify tumors at different stages of tumorigenesis and to examine where spontaneous tumors initiate (Momota and Holland, 2005; Hawes and Reilly, 2010). A transgenic mouse has been developed in which two oncogenes, encoding $P53^{R172H}$ and $KRAS^{G12D}$, are expressed together with two reporter genes, encoding enhanced green fluorescent protein (EGFP) and firefly luciferase, in a single open reading frame following Cre-mediated DNA excision. Systemic administration of adenovirus encoding Cre to these mice induced specific transgene expression in the liver during hepatocellular adenomas (Ju HL *et al*., 2015).

Recently, the Tau mutation A152T was described as a novel risk factor for frontotemporal dementia spectrum disorders and Alzheimer disease. A mouse model expressing human full-length Tau with this mutation (hTau40(AT)) has been generated to study the effects of this mutation. These mice are suitable for mechanistic studies of Tau induced toxicity and *in vivo* validation of neuroprotective compounds (Sydow *et al*., 2016).

On the basis of the knowledge that the activity of the nuclear factor-Y (NF-Y) transcription factor is restricted *in vitro* to proliferating cells, the group in which I have performed my PhD studies has generated a transgenic reporter mouse, called MITO-Luc (MITO stands for mitosis and Luc for luciferase), in which an NF-Y–dependent promoter controls luciferase expression. In these mice, BLI of NF-Y activity visualizes areas of physiological cell proliferation and regeneration during response to injury. Using this tool, for the first time a role of NF-Y activity on hepatocyte proliferation during liver regeneration has been highlight. MITO-Luc reporter mice should facilitate investigations into the involvement of genes in cell proliferation and provide a useful model for studying aberrant proliferation in disease pathogenesis. They should be also useful in the development of new anti/pro-proliferative drugs and assessment of their efficacy and side effects on non-target tissues (Goeman *et al*., 2012). Recently, it has been demonstrated that *in vivo* imaging of NF-Y proliferation marker in MITO-Luc reporter mice is capable of measuring the reduction of cell proliferation due to genotoxic/apoptotic agents, γ rays or antineoplastic drugs, or the increased proliferation associated with the inflammatory and regenerative reactions occurring after a toxic insult (Rizzi *et al*., 2015). These data provide a novel way to translate the evidence of toxic effects obtained in preclinical animal studies, by the direct, noninvasive measure of dividing cells in humans.

Contrary to what has been published for mouse models, there are still few transgenic zebrafish models that exploit BLI by driving the expression of luciferase reporter under the control of a regulatory sequence. Up today the BLI technology has been mainly applied to zebrafish tumor xenograft model, using luciferase labeled cancer cells to track tumor growth *in vivo* and to test the efficacy of antitumor and antiangiogenic compounds (Zhao *et al*., 2009). Worthily, Chen's group, for the first time, has applied BLI methodology in a transgenic zebrafish model. Both ubiquitous and tissue-specific luciferase-based transgenic lines has been described. In the ubiquitous lines ubiquitin (ubi) or β-actin2 promoters drive widespread luciferase expression. In the tissue specific lines cryaa or cmlc2 promoters drive luciferase expression specifically in the lens or cardiomyocytes, respectively (Chen *et al*., 2013). In the cml2-luc line, authors show that luciferase-based live imaging reliably estimates muscle quantity in an internal organ, the heart, and can longitudinally follow cardiac regeneration in individual animals after major injury.

Transgenic mouse models designed to recapitulate genetic and pathologic aspects of cancer are useful to study early stages of disease as well as its progression. Among several, two of the most sophisticated models for pancreatic ductal adenocarcinoma (PDAC) are the LSL-Kras$^{G12D/+}$;Pdx-1-Cre (KC) and LSL-Kras$^{G12D/+}$;LSL-Trp53$^{R172H/+}$;Pdx-1-Cre (KPC) mice, in which the Cre-recombinase regulated by a pancreas-specific promoter activates the expression of oncogenic Kras alone or in combination with a mutant p53, respectively. During my PhD thesis I have developed and characterized two novel disease models MITO-Luc-KC- and -KPC mice, obtained through intercross with our MITO-Luc mouse model, engineered to express the luciferase reporter gene in cells undergoing active proliferation. In these mice we have had the opportunity to follow PDAC evolution in the living animal in a time frame process. Altogether, *in vivo* and *ex vivo* analyses demonstrate that MKPC and MKC mouse models are powerful tools for visualizing PDAC development in terms of proliferation in the entire living animal in a spatio-temporal manner. Most notably, these results also demonstrate that, in these mouse models, it is possible to identify early steps of pancreatic carcinogenesis noninvasively in living animals in which proliferation events take place before tumour appearance. From a pharmacological point of view, this opens the possibility to design therapeutic protocols with a more precise timing than those using the tumour palpability as a starting point, a parameter of low specificity and sensitivity. Moreover, from an ethical point of view, application of BLI technique offers interesting additive values, too. Indeed, the analysis is carried out on the same living animal with a series of imaging sessions comfortable for the subject. Most important, this technique allows longitudinal experiments without sacrificing groups of mice at each time point thus reducing the necessary number of animals (de Latouliere *et al*., 2015). At the end of the thesis this paper has been placed as attach.

Parallel to the above described mouse models, during my PhD thesis I have also developed a reporter transgenic zebrafish model in which, using the activity of the master regulator of proliferation, NF-Y, it is possible to visualize proliferation in intact animals. As a sensor of NF-Y transcriptional activity, we used, as in MITO-Luc mice (Goeman *et al*., 2012), a cyclinB2 promoter fragment driving transcription of luciferase and GFP genes. The new transgenic zebrafish model, called MITO-Luc-GFP Zebrafish, is a remarkable tool for following NF-Y transcriptional activity *in vivo*, allowing the monitoring of active cell proliferation in longitudinal studies both during embryonic stage and during the entire animal life. The presence of GFP and luciferase as reporters in these animals makes highly versatile our tool, thus consenting to choose the most appropriated method of analysis according to the experimental issue should be addressed (confocal analysis and/or BLI technique) overcoming the major limitations and exploiting the advantages of each method. The development and characterization of this animal model, reporter for proliferation, will be the subject of my dissertation.

4. INTRODUCTION

4.1. Zebrafish as a versatile tool for biological research

Zebrafish (*Danio rerio*) is native to rivers of Southeast Asia, reaches 4 cm in length and lives up to 5 years. Zebrafish models allow to perform genetic analysis and combine the advantages of invertebrates (e.g: *D. melanogaster* and *C. elegans*), which can be subjected to large-scale mutagenesis and chemical screening, and vertebrates such as the mouse, which shows more similarities to human.

Zebrafish models represent a critical step to improve treatments of malignant diseases, among which cancer, as an intermediate method of experimentation between cell culture based assays and human clinical trials. This is due to the small size, embryos optical transparency, low maintenance cost, high fecundity and rapid development. Furthermore despite 450 million years of evolutionary distance, cell and molecular pathogenesis that govern vertebrate development including signaling, proliferation, differentiation and apoptosis are highly conserved between human and Zebrafish. Approximately 70% of all human disease genes have functional homologs with Zebrafish (Santoriello and Zon, 2012). The complete genomic sequence and various tools for genetic manipulation are available. Additionally, great tissue regeneration ability make Zebrafish a suitable tool for studying the wound healing response to various injuries (Niethammer *et al*., 2009).

Thousands of Zebrafish can be housed in a laboratory with low husbandry costs. Breeding pairs can produce over 200 embryos each week that are fertilized outside of the mother and can be easily collected from the breeding tank. Embryonic development from a single cell, and the rapid formation of discrete tissues and organs can be easily analyzed (Kimmel *et al*., 1995). In this context, the use of fluorescent proteins, that allows the study of disease processes, and the identification of the corresponding defective genes, are particularly advantageous. (Spitsbergen, 2007). On this basis several mutant and transgenic lines have been generated, in order to shed light on the genes and/or molecular mechanisms involved in pathologic events (Detrich, 2008). Although fluorescent reporters are valuable optical tools for real-time imaging in transparent zebrafish embryos, they are not useful in living adult animals since the expression of fluorescent proteins is not *in vivo* detectable in most of the tissues during adulthood. This is due both to the no-transparent skin of adult Zebrafish that make difficult to detect signals from an internal organ and to a low signal-to-noise ratio, except for cells that are close to the body surface.

Based on these considerations, the aim of a project that I performed during PhD period has been the establishment of a transgenic zebrafish model that could allow to follow physiological and/or pathological processes characterized by active cell proliferation in the embryo as well as in

the adult. So that we have developed a new transgenic zebrafish line in which the luciferase reporter gene are placed under the control of a cyclinB2 minimal promoter tightly regulated by the transcription factor NF-Y, which we have named MITO-Luc-GFP zebrafish model to visualise proliferation events in living animals via noninvasive BioLuminescenceImaging (BLI) technology.

The use of BLI on our MITO-Luc-GFP zebrafish model could be an accurate indicator of active cell proliferation in longitudinal studies during the entire animal life. We predict that MITO-Luc-GFP zebrafish model will be useful to readily and easily measure cell proliferation for several experimental applications, ranging from oncology to regenerative medicine, for testing the efficacy of old and/or new drugs. A large progeny can be generated in a short time and screened by BLI for large-scale drugs such as pharmacological compounds. Finally, in oncological research, our zebrafish model, if crossed with tumor model lines, would allow quantitative measurements of tumor progression, metastasis and treatment response.

4.2. Oncological research

The role of Zebrafish as vertebrate model organism in several areas of cancer research has increased over the last decades. Its use has been applied mainly in the establishment of cancer models, evaluation of tumor angiogenesis, study of tumor metastasis, anti-tumor drug screening and drug toxicity evaluation (Zhao *et al*., 2015).

Spontaneous neoplasia was rarely found in wild Zebrafish. However, using a combination of chemical treatment, genetic technology, and tumor cell xenotransplantation, the vast majority of human tumors can be modeled in Zebrafish (Feitsma and Cuppen, 2008). For example, carcinogenic chemical treatment is commonly used in inducing tumorigenesis in Zebrafish (Mirbahai *et al*., 2011). Moreover, a comprehensive collection of reverse genetics tools, has been developed for studying function of genes involved in carcinogenesis in this organism. Among these tools, morpholinos are usually injected at the 1-4 cell stage of embryos to provide transient knockdown of the target gene expression (Heasman, 2002). Another targeted genome modification technology, called TILLING (Targeting Induced Local Lesions IN Genomes), is highly dependent on large-scale traditional post-transcriptional forward genetic screens expression and pseudo-typed retrovirus mediated insertional mutagenesis (Kuroyanagi *et al*., 2013). Engineered endonucleases, including ZFNs (zinc finger nucleases), TALENs (transcription activator-like effector nucleases), and the CRISPR-Cas system, provide efficient strategies to disrupt site-directed genes by inducing double strand breaks in the target genes (Shah *et al*., 2015; Huang *et al*., 2012). Among genetic technology there is transgenic expression of human or mouse oncogenes, that has allow the establishment in Zebrafish of several cancer models (Lu *et al*., 2015; Ju B. *et al*., 2015). Finally, xenotransplantation

represents a novel method to establish tumor models in Zebrafish (Veinotte *et al*., 2014; Barriuso *et al*., 2015). One of the great strengths of xenotransplantation is that the transplanted tumor cells can be marked by fluorescent staining to enable them to be distinguished from normal cells in order to allow clear observation of the development process of the tumor (Bentley *et al*., 2015).

4.3. Drug screening in Zebrafish

The high fertility and low maintenance costs of Zebrafish makes this animal model suitable for the large-scale screen of antineoplastic drug efficacy and toxicity.

The effects of antineoplastic drugs have often been detected by biochemical assays or in cell line models. Nevertheless due to the absence of a complete biologic context in the screening process, the identified active compounds were often ineffective when applied in a vertebrate model. A whole animal screen sheds valuable information on anti-tumor effects, organ toxicity, and pharmacokinetic data based on the entire organism (Ghotra *et al*., 2012). While, mice are fisically prohibitive for large-scale screen, Zebrafish have emerged as a powerful platform for use in high-throughput antineoplastic drug screening on the strength of the following advantages. In fact, a pair of Zebrafish produce hundreds of embryos a week, and they have a small size that can be arrayed in a 96-well plate, which greatly decreases the cost of maintaining them in the laboratory.

Many small molecule libraries are made up of compounds with known biological function, allowing rapid elucidation of biological pathways within the organism. In Zebrafish, drug treatments can be easily achieved by merely adding the medicine to the aqueous environment. Chemical treatment can occur at any point during development or in the adult organism and chemical dosage can be controlled, which can be advantageous when studying essential functions (Taylor *et al*., 2010). In addition, the transparent zebrafish embryo enables the real-time noninvasive imaging of anti-tumor effects and drug toxicity.

In the first chemical screen in Zebrafish, 1,100 compounds selected from the DIVERSet E Library (Peterson *et al*., 2000) have been screened in 96-well plates for small molecules that caused developmental phenotypes during the first three days of development. Next, 16.320-compound from the same library have been screened in zebrafish embryos for alterations of histon3 phosphorylation during cell cycle. This screen revealed 14 compounds that had not been previously identified as having cell cycle activity despite numerous mitotic screens of the same library with mammalian cell lines. (Murphey *et al*., 2006). Later, anti-angiogenesis drugs have been screened in Zebrafish. Following a screen of 288 new compounds, two kinase inhibitor compounds were found to have anti-angiogenic properties and a phosphorylase kinase subunit G1 (PhKG1) was identified as the kinase target (Camus *et al*., 2012).

4.4. MITO-Luc-GFP zebrafish model

Noninvasive BLI has been widely used in mice for monitoring gene expression (Bu *et al*., 2013), bacterial and viral infections (Signore *et al*., 2010), as well as cell proliferation and transformation (Goeman *et al*., 2012, Rizzi *et al*, 2015; de Latouliere *et al*., 2015). These tools offer the advantage of noninvasive *in vivo* assessment of the molecular and cellular events that are often targets of therapy; as such, these events can be studied in individual animals over time. This reduces the number of animals required for a given study and improves the data set, as the temporal data, allowing for each animal to serve as its own internal control. For small rodents, such as mice, this noninvasive imaging technique allows detection of signals throughout the entire animal (Signore *et al*., 2010). It has been recently generated a mouse model which allows to visualize through BLI any proliferation events in the context of the entire alive animals during development and adult life, called MITO-Luc reporter mice. In these mice the luciferase reporter gene are placed under the control of a cyclinB2 minimal promoter containing three CCAAT boxes conserved between mouse and human and tightly regulated by the transcription factor NF-Y (Goeman *et al*. 2012).

The nuclear factor-Y (NF-Y) is a trimeric activator composed of NF-YA, NF-YB, and NF-YC subunits, all of which are required for DNA binding. The three subunits are highly conserved in evolution and represent the complex recognizing the CCAAT motif (Dolfini *et al*., 2009). The NF-Y complex supports proliferation regulating the basal transcription of regulatory genes responsible for cell cycle progression, among which are mitotic cyclin complexes and it exerts its activity only in proliferating cells (Bolognese *et al*., 1999; Caretti *et al*., 1999; Farina *et al*., 1999; Sciortino *et al*., 2001; Gurtner *et al*., 2003, 2008; Di Agostino *et al*., 2006; Gatta *et al*, 2011). Previously we provide evidence that NF-Y plays a central role in the switch from proliferation to differentiation. In proliferating skeletal muscle cells, all subunits are expressed, whereas in terminally differentiated cells, NF-YA is undetectable, and the suppression of NF-Y function is crucial for the inhibition of multiple cell cycle genes and the induction of early muscle differentiation markers (Farina *et al*., 1999; Gurtner *et al*., 2003; Gurtner *et al*., 2008; Manni *et al*., 2008). In line with this, conditional deletion of NF-YA in mice causes early embryo lethality, demonstrating that NF-Y is essential for early mouse development (Bhattacharya *et al*., 2003). Moreover, it has been described that inhibition of NF-Y function leads to defects in embryonic (ES) and hematopoietic (HSC) stem cell proliferation (Grskovic *et al*., 2007; Bungartz *et al*., 2012).

Two of the three CCAAT boxes of the cyclinB2 minimal promoter used to generate MITO-Luc reporter mice are conserved in Zebrafish (Fig.2A). Moreover, the three NF-Y subunits are highly conserved between mouse, human and Zebrafish (Fig.2B). This indicates that mouse

cyclinB2 promoter region may be sensitive to NF-Y activity in Zebrafish, too. Since NF-Y exerts its activity only in proliferating cells, this model could provide an accurate measure of active cell proliferation not only in mouse but also in Zebrafish. To date, the only examples of zebrafish luciferase reporter models have been described by Chen's group in the last 2013. The authors have described both ubiquitous and tissue-specific luciferase-based transgenic lines. In the ubiquitous lines, ubiquitin (ubi) or β-actin2 promoters drive widespread luciferase expression. In the tissue specific lines, cryaa or cmlc2 promoters drive luciferase expression specifically in the lens or cardiomyocytes, respectively (Chen *et al* 2013). Although not based on transgenesis, another example of optical *in vivo* imaging, based on fluorescent protein in Zebrafish, is the use of GFP transfected stem cells transplanted in the casper strain that maintains relative transparency throughout life (White *et al.*, 2008). This enables noninvasive quantitative assessment of engraftment in live animals, and identification of colonization and proliferation sites for these cells (Heilmann *et al*., 2015).

Here we report the production of a new zebrafish model to visualize, by BLI, proliferation events in the context of the whole animal both during development and adult life. In this transgenic line, luciferase and GFP reporter genes are placed under control of cyclinB2 minimal promoter. The use of BLI on our zebrafish model as read out for proliferation events would speed up in the future the evaluation of anti- or pro-proliferative drug candidates.

A

Murine cyclinB2

agacaaggaaacaacaaagcctggtggcctcgctggttgct
atgacaagcaaatacaagccag**ccaat**caacgtgcagaaag
gccttccagtctag**ccaat**gggttgcgcgcgccctgcgtgc
gtctac**ccaat**agtgcgtcagcggcgc+1ATGGCGCTGCTC
CGACGCCCGACG

Zebrafish cyclinB2 like

taagcgccgcctctcttttcat**ccaat**cgaactctagtatt
tcccgagccagtga**ccaat**cagagaacgcagagcggtattt
gaatcaccagcaggcctttgtactgtatacgcacggcttgt
tattagttgagttggacgagaaacgcc+1ATGGAAATGCAC
GCTCTG

B

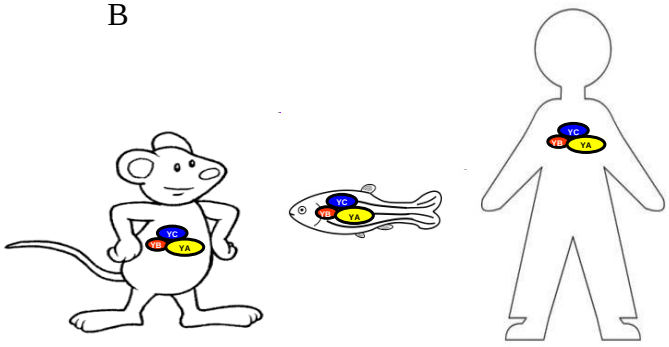

Figure 2: ***MITO-Luc-GFP zebrafish model*** **(A)** confront of cyclinB2 minimal promoter sequence in mice and Zebrafish: two of the three CCAAT boxes of mice are conserved in Zebrafish. **(B)** Schematic representation of the three NF-Y subunits, highly conserved between mouse, human and Zebrafish.

5. RESULTS

5.1. Establishing a Tg (cyclinB2:Luc-GFP) zebrafish line

To develop a zebrafish model to visualize by optical imaging proliferation events in the context of the whole animal, a 312 bp fragment of the murine cyclinB2 promoter was cloned upstream the in frame sequences of firefly luciferase (Luc) and GFP reporter gene within the zebrafish Tol2 transposable element pT2KXIG plasmid (Fig.3A).The resulting pT2KXIGΔin-cylinB2-Luc-GFP construct and, as control, the pT2KXIGΔin-Luc-GFP empty construct were transiently injected into one to four-cell stage wild type AB strain embryos. *In vitro* luciferase activity assay performed in lysates showed 80 fold increased transcriptional activity from pT2KXIGΔin-cylinB2-Luc-GFP than the pT2KXIGΔin-Luc-GFP transformed embryos (Fig.3B). These experiments demonstrate a cyclinB2 promoter- dependent luciferase expression in zebrafish embryos.

Next, to generate stable lines, the pT2KXIGΔin-cylinB2-Luc-GFP construct and Transposase mRNA were co-injected into one to four-cell stage AB strain embryos. Transgenic founders were collected by a GFP fluorescence microscopy analysis. Two independent transgenic zebrafish lines were obtained and named MITO-Luc-GFP[1] and MITO-Luc-GFP[2] zebrafish model. Quantitative PCR analysis with genomic DNA from whole embryos has shown clear differences in the transgene copies in the two lines (Fig.3C). Due to the different number of inserted transgenes, MITO-Luc-GFP[1] shown more fluorescence than MITO-Luc-GFP[2] (Fig.3D). *In vitro* luciferase activity assay confirmed this results (Fig.3E). In particular, through inverse PCR (Fig.3F) a single insertion of MITO-Luc-GFP[2] Zebrafish transgene has been localized in the first intron of the prkag2a gene protein kinase, AMP-activated, gamma 2 non-catalytic subunit a on Chromosome 24, position (28.173.305-28.302.316) (ZFIN Gbrowse).

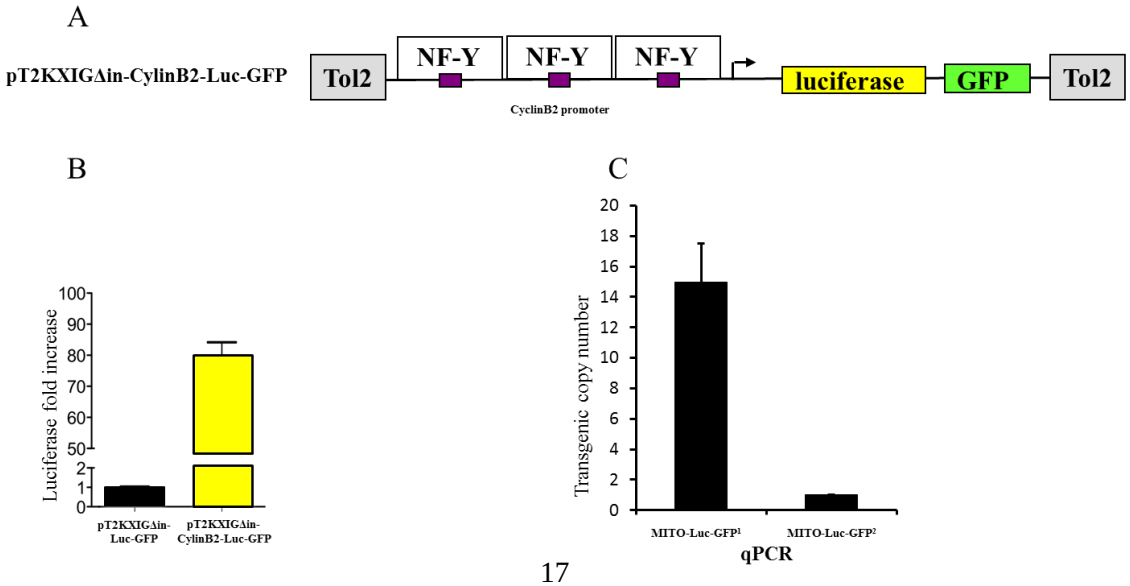

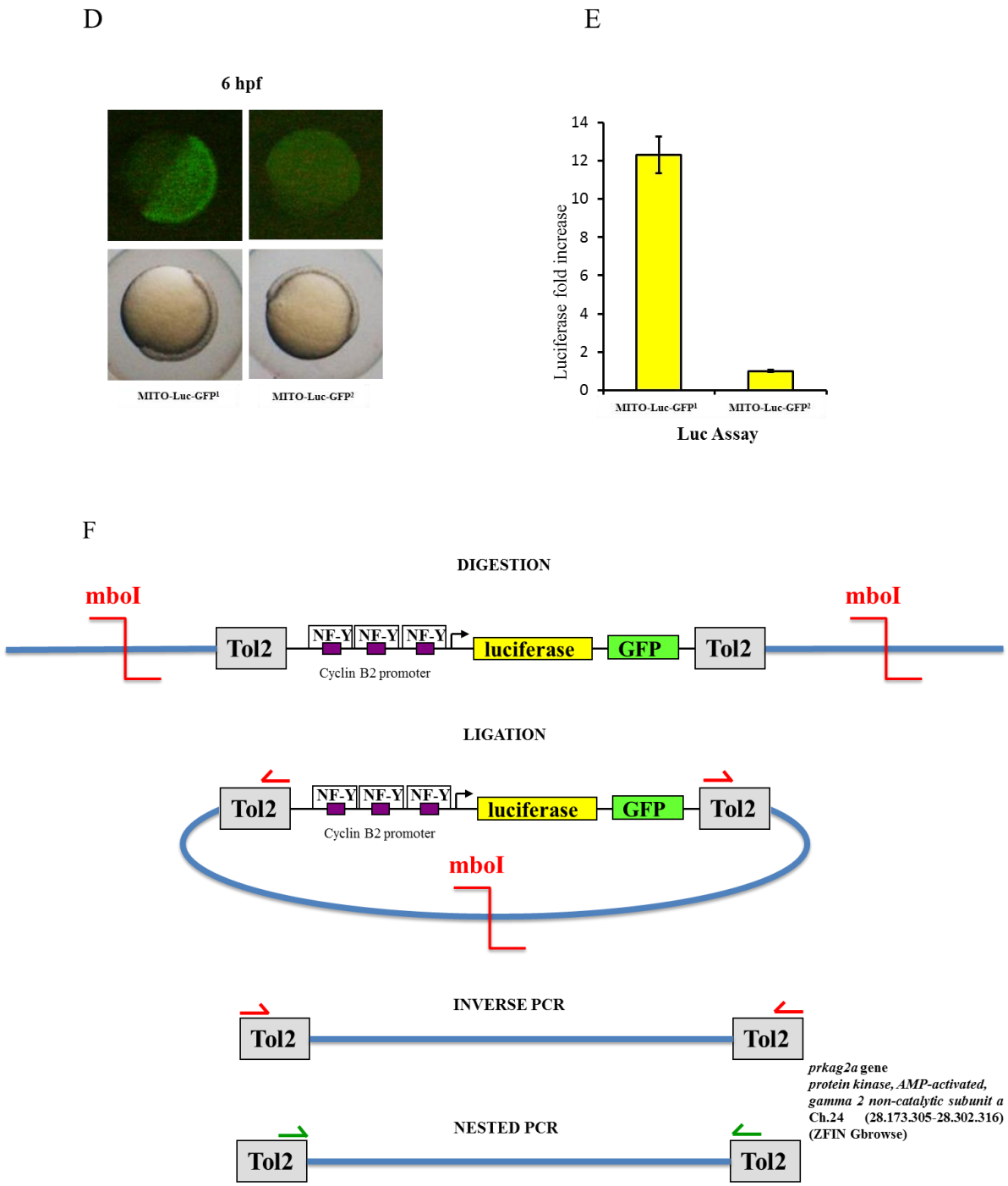

Figure 3. ***Establishing a Tg (cyclinB2:Luc-GFP) zebrafish lines.*** **(A)** Diagram of the Tg (cyclinB2:Luc:GFP) expression vector. A fragment of murine cyclinB2 promoter (violet) was cloned upstream of the firefly luciferase gene (yellow) and the green fluorescent protein GFP (green), in the pT2KXIGΔin plasmid containing the Tol 2 transposable element (gray). **(B)** One to four-cell stage AB strain embryos were transiently injected with the pT2KXIGΔin-Luc-GFP (black bar) or the pT2KXIGΔin-cylinB2-Luc-GFP (yellow bar). The error bars are mean standard deviations from three experiments performed in triplicate. **(C)** Relative quantification of transgene copy number in MITO-Luc-GFP zebrafish lines by qPCR. The error bars are mean standard deviations from two experiments performed in triplicate. **(D)** GFP expression in 6 hpf embryos MITO-Luc-GFP zebrafish lines. **(E)** Relative luciferase activity in MITO-Luc-GFP$^{1/2}$ zebrafish lines. The error bars are mean standard deviations from three experiments performed in triplicate. **(F)** Schematic representation of Inverse PCR protocols.

5.2. *Analysis of GFP expression*

GFP expression was observed in 6, 24 and 33 hour post fertilization (hpf) embryos by confocal microscopy from MITO-Luc-GFP[1] transgenic lines (Fig.4). Interestingly, in early stages (Fig.4A,B) the GFP expression is almost ubiquitous throughout the embryos while it appears to be much more tissue specific in 33 hpf embryos being accumulated in the head, proximal trunk and in developing fin (Fig.4C, arrows). Interestingly, this picture recapitulates published data obtained in 20-40 hpf embryos exposed to BrdU where labeling was mostly observed in the central nervous system and in the developing fin (Laguerre *et al*., 2005).

To start to evaluate the reliability of MITO-Luc-GFP zebrafish model as tool to visualize cell proliferation through GFP fluorescent signal, we have imaged living whole-mount embryos at different stages of development. Embryos were dechorionated and agarose embedded. Once mounted, 4 hpf embryos were imaged, using confocal microscope, every 4 min for 1,3 hrs while 19 hpf embryos were imaged every 25 min for 15 hrs. Movies were achieved by merging sequential time laps acquisition. Individual cells can be identified, and several layers of the tissue can be distinguished. In 4hpf embryos the migration of embryonic tissue is visible (Fig.4H and movie 1 embedded in the CD). In this stage, characterized by a 30%-epiboly, the morphogenetic cell movements of involution, convergence, and extension occur (Fig.4H, arrows), producing the primary germ layers and the embryonic axis (Kimmel *et al*., 1995). In 19 hpf embryos the somite development is visible. In this stage, anterior somites develop earlier than posterior ones. The notochord becomes more distinguishable from the ventral part of the neural keel, the rudiments of the primary organs become visible. Morphogenesis associated with the previous constriction of the yolk begins to straighten out the posterior trunk, producing an increase in the length of the embryo in collaboration with the development of the tail (Kimmel *et al.*, 1995) (Fig.4I and movie 2 embedded in the CD). The extension of the tail to elongate the embryo is covered by the presence of the agarose that avoid the straightening of the tail.

It is important to take in mind that a bias of these experiments can reside in the stability of GFP protein that has a half-life of approximately 26 hrs (Corish and Tyler-Smith, 1999). Thus, once GFP is expressed the fluorescent signal persists and a cell is green labeled during this period of time. The long GFP protein half-life can partially masks the exact dynamic of proliferation events occurring during zebrafish embryogenesis.

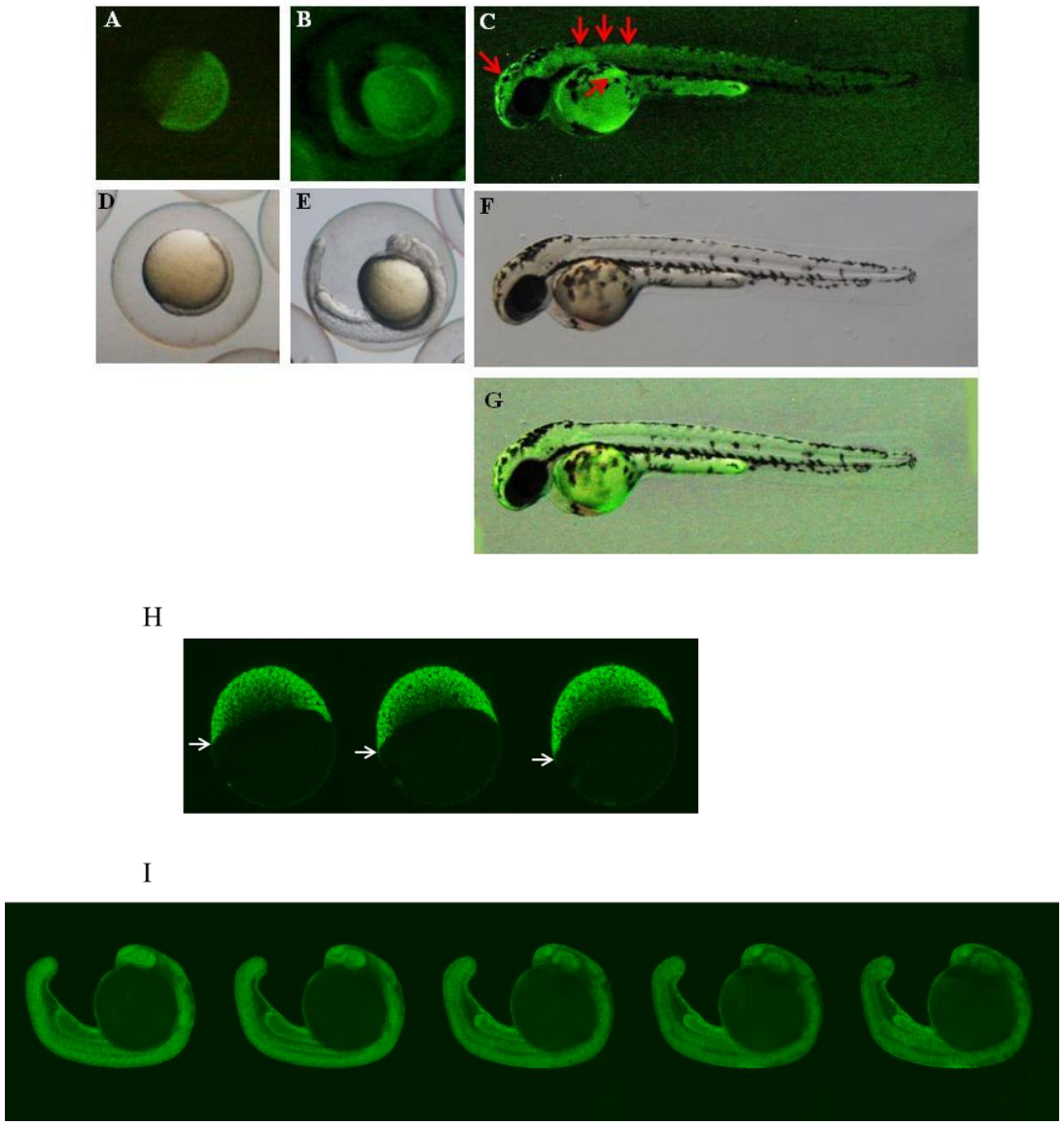

Figure 4. ***GFP expression.*** **(A)** 6**, (B)** 24 and **(C)** 33 hpf **e**mbryos were imaged by ST2 Leica stereomicroscope with high resolution CCD camera for GFP signal **(A-C)**, or bright light **(D-F)**. **(G)** Merge of GFP signal and bright light in 33 hpf. **(H)** Representative frame of time laps acquisition of 4 hpf MITO-Luc-GFP[1] embryogenesis (arrows) imaged every 4 min for 1,3 hrs using a Zeiss confocal microscope. **(I)** Representative frame of time laps acquisition of 19 hpf MITO-Luc-GFP[1] embryogenesis imaged every 25 min for 15 hrs using confocal microscope.

Movie 1. Time laps acquisition of 4 hpf MITO-Luc-GFP embryogenesis imaged every 4 min for 1,3 hrs using a confocal microscope.

Movie 2. Time laps acquisition of 19 hpf MITO-Luc-GFP embryogenesis imaged every 25 min for 15 hrs using a Zeiss confocal microscope.

5.3. Analysis of Luciferase expression

To start to establish weather MITO-Luc-GFP zebrafish model could be useful to visualize by BLI physiological proliferation events in the context of whole animals, both during development and adult life; embryos, juveniles and adults MITO-Luc-GFP$^{1/2}$ Zebrafish were collected, anesthetized, bathed in d-luciferin and *in vivo* imaged (Fig.5). Light signal emitted by individual embryos ($8{,}03E^{+06} \pm 1{,}21E^{+06}$) (Fig.5A) is higher than those emitted by juvenile ($5{,}21E^{+05} \pm 0{,}78E^{+05}$) (Fig.5B) and adult ($6{,}10E^{+05} \pm 0{,}92E^{+05}$) animals (Fig.5C). This result is consistent with the pervasive cell proliferation in embryos, while it is much more tissue specific in juveniles and adults. In agreement with this signal is widespread on embryos, while it is localized in the abdominal part of the juvenile and adult animals. Interestingly, kidney is present in this region and this organ is recognized as a site of active proliferation being target of stem cell colonization and active hematopoietic regeneration in adult Zebrafish. Although other experiments are needed to elucidate in detail which abdominal organ/s is/are the source of light, this evidence suggest that luciferase activity in MITO-Luc-GFP Zebrafish might be an useful toll to spatio/temporally visualize cell proliferation events.

Next, luciferase activity was measured in embryo, juvenile and adult homogenates from MITO-Luc-GFP^{1} zebrafish line. Embryo, juvenile and adult homogenates of AB zebrafish line were used as negative control. The *in vitro* results closely resembled those seen *in vivo* (Fig.5D), being luciferase activity higher in embryo than in juvenile and adult homogenates. Unexpected, luciferase activity results bigger in juveniles than adults. This discrepancy with *in vivo* results can be explained considering proliferation/total tissue ratio. In fact, being juveniles little than adults, in *in vitro* experiments, proliferating cells are less diluted in the homogenates from the entire animal. This do not happen in *in vivo* experiments, where only the signal coming from proliferating tissue is considered. MITO-Luc-GFP^{2} zebrafish line showed similar *in vivo* and *in vitro* results but with lower intensities (not shown), due to its lower transgene copy number.

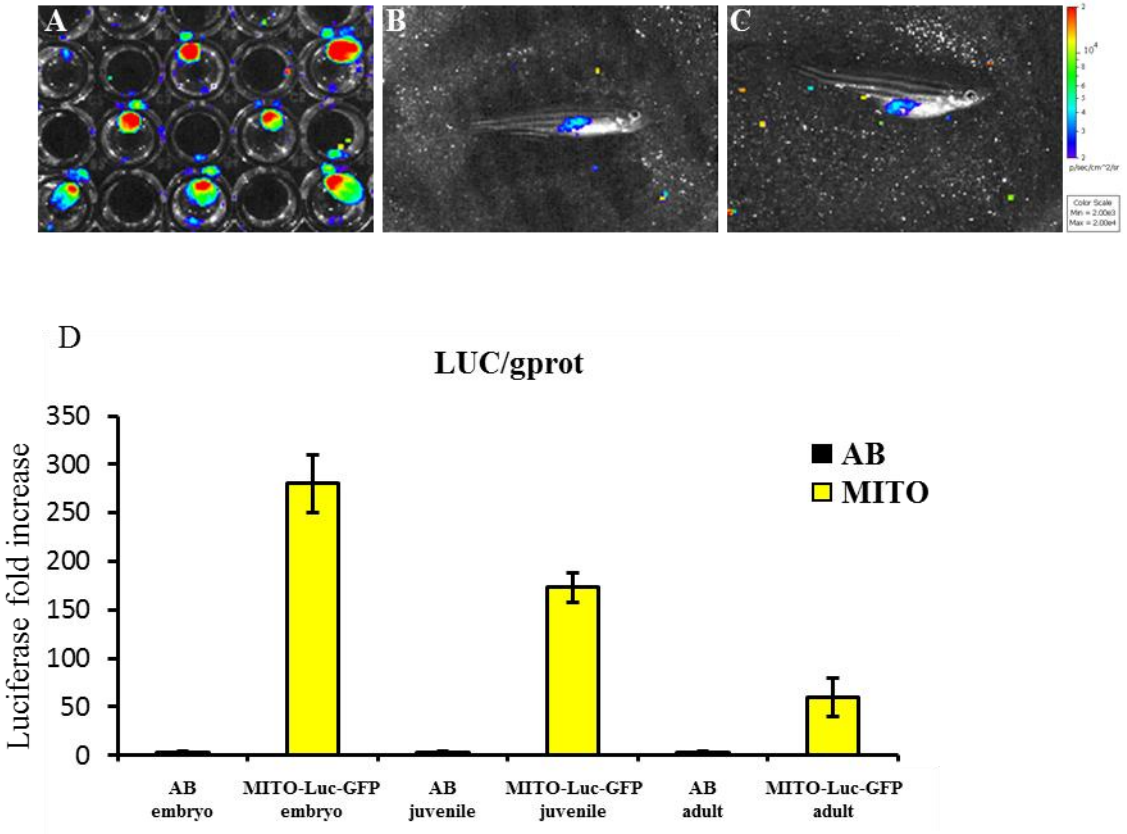

Figure 5. ***Luciferase expression.*** **(A-C)** BLI of representative MITO-Luc-GFP Zebrafish at embryos **(A)**, juvenile **(B)** and adult **(C)** stages. Light emitted from the animal appears in pseudocolor scaling. **(D)** Luciferase activity of homogenates of embryos, juveniles and adults from MITO-Luc-GFP line (yellow bar) and AB line (black bar) as control. The error bars are mean standard deviations from three experiments performed in triplicate.

5.4. *Histological Analysis: GFP and Luciferase expression in proliferating cells*

To verify that MITO-Luc-GFP[1] zebrafish model could be suitable means to identify cell proliferation events by monitoring both reporter expressions, the cellular distribution of GFP and luciferase was analysed by immunofluorescence (Fig.6). Luciferase and GFP signals were merged with nuclei staining by DAPI and were observed in almost all nuclei in distal trunk section of 24 hpf embryos (Fig.6A,B). Interestingly, a comparable localization of GFP and luciferase were observed in adult epidermal fin tissue (Fig.6F,G,H). Remarkably, several GFP positive cells also express the proliferation marker phosphorylated histone 3 isoform (pH3) (Fig.6C,D,E), a well-known marker of mitosis (Hendzel *et al.*, 1997). As the same, GFP positive cells in intestine (Fig.6I) and ovary (Fig.6M) also express PCNA (Fig.6J,K,N,O) another well-documented marker for cell proliferation in zebrafish (Kassen *et al* 2008**)**. Although several GFP positive cells are also positive for proliferation markers, not all of them do it. One possible explanation is due to the longer half-life of GFP protein (26hr) compared with that of luciferase, pH3 and PCNA.

Next, adjacent slices from testis, intestine, gills and kidney, of adult MITO-Luc-GFP[1] line were stained with antibodies against luciferase, pH3 or PCNA (Fig.7). As expected, PCNA is expressed in proliferating spermatogonia of the testis (Fig.7D) and in mucosa of intestinal villi (Fig.7B). pH3 is expressed in filament and in gills lamellae (Fig.7H, arrows) and in the proximal tubule of the nephron in the kidney section (Fig.7F). Of note, throughout all tissue analysed, cells expressing proliferation markers, either PCNA or pH3, show immunoreactivity for luciferase (Fig.7A,C,E,G), indicating that MITO-Luc-GFP reporter zebrafish is a powerful tool for visualizing proliferation events in live animals. In gill sections most of the cells labelled with antibodies against luciferase or GFP were stained by the antibody against pH3 (Fig.7G,H,I) , but not all of them. This unexpected expression pattern, which was not observed with PCNA expression, is due to ability of pH3 to stain only mitotic cells and not proliferating cells in other cell cycle phases.

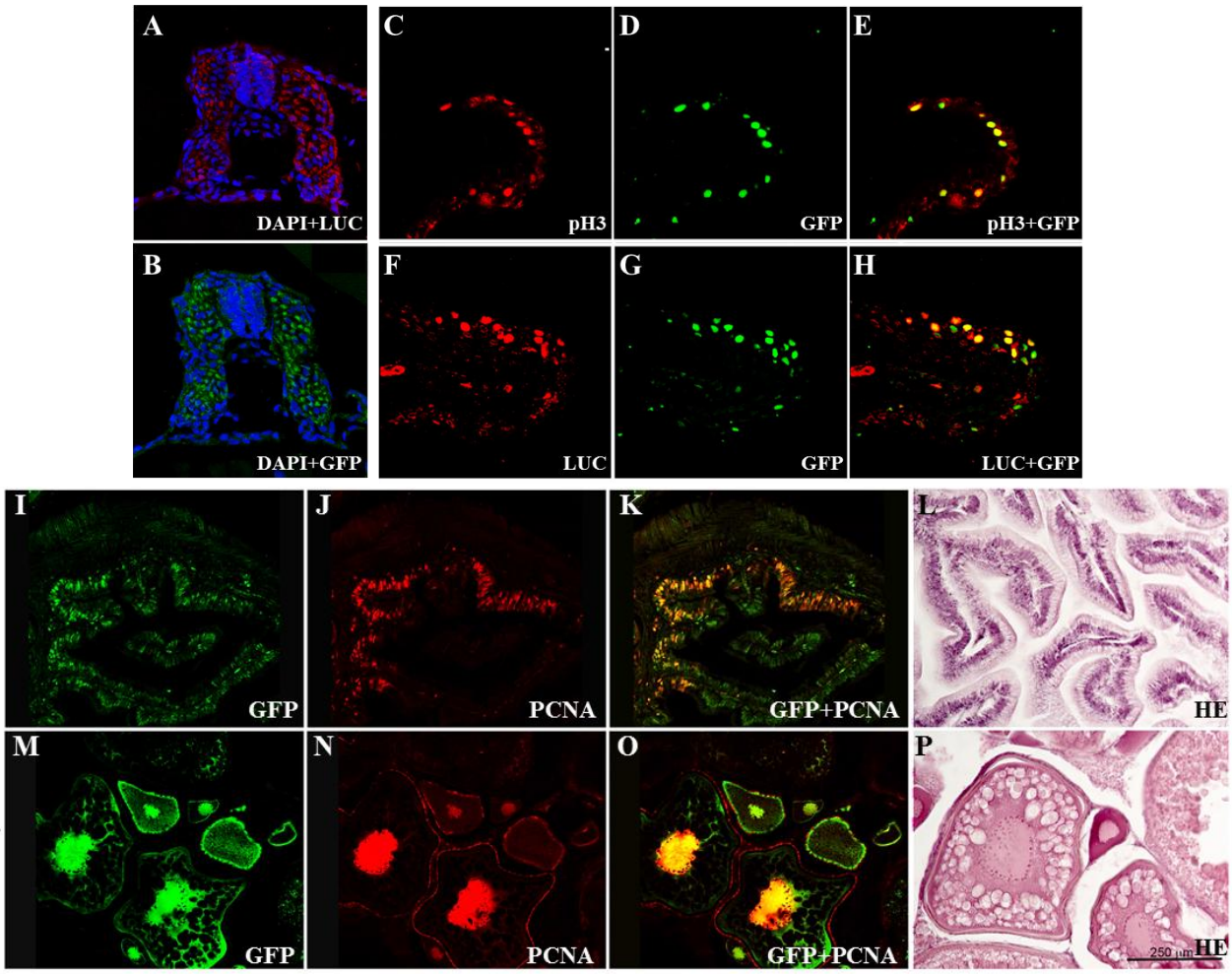

Figure 6. ***Immunofluorescence analysis: GFP and Luciferase expression in proliferating cells.*** Immunofluorescence analysis of luciferase **(A)** and GFP **(B)** Dapi merge in 24 hpf embryo trunk. Immunofluorescence analysis of pH3 **(C),** luciferase **(F)**, GFP **(D, G)**, pH3-GFP merge **(E)** and luciferase-GFP merge **(H)** in adult epidermal tissue. Immunofluorescence analysis of intestine **(I-K)** and ovary **(M-O)**. GFP **(I, M)**, PCNA **(J, N)**, GFP-PCNA merge **(K, O)** and HE staining **(L, P)**are shown.

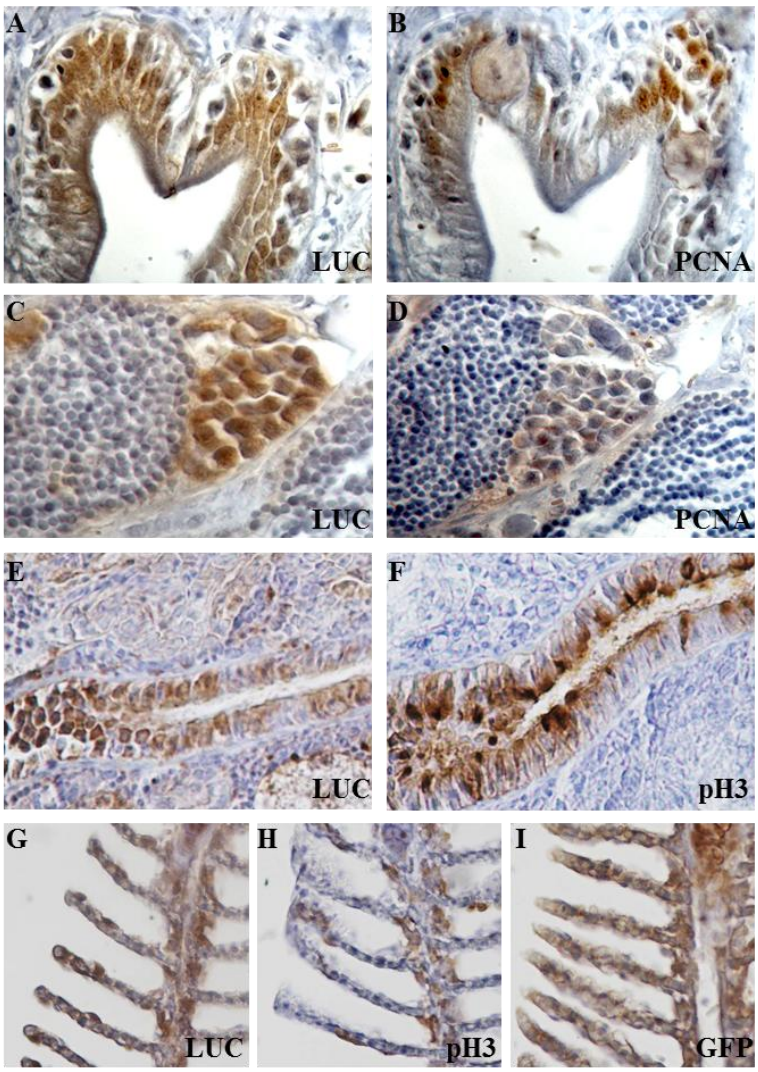

Figure 7. ***Immunohistochemical analysis: GFP and Luciferase expression in proliferating cells.*** Immunohistochemical analysis of luciferase **(A, C, E, G)**, PCNA **(B, D)**, pH3 **(F, H)** and GFP **(I)** in adult intestine **(A, B)**, testis **(C, D)**, kidney **(E, F)** and gills **(G, H, I)**.

5.5. Caudal fin regeneration in MITO-Luc-GFP animals.

To investigate whether MITO-Luc-GFP zebrafish model could be a powerful tool to visualize induction of proliferation by monitoring GFP or luciferase gene expression we took advantage of Zebrafish ability to regenerate amputated fins, a process based on cell proliferation (Ivanova *et al*., 2014). Briefly, the expression of GFP has been imagined during regeneration of caudal fin in 3 dpf (days post fertilization) MITO-Luc-GFP$^{1/2}$ embryos after fin clip treatment. Embryos were subjected to the cut of the last part of the caudal fin, embedded in agarose and pictures were captured every 15 min for 14 hrs by confocal microscope. Movies were achieved by merging sequential time laps acquisition allowing the monitoring of the regeneration of the last part

of the tail. A proliferating GFP labeled cell cohort is observable. A rapid migration of epidermal cells to protect the wound is visible. Fluorescent/proliferating cell movement occurs to replace the wound epidermis with a new scar tissue (movie 3 and 4 embedded in CD). Some frames are reported to summarize the process of regeneration (Fig.8A,B).

Next, we have applied BLI to monitor the progress of caudal fin regeneration in adults subjected to fin clip treatment (Fig.8C-H). MITO-Luc-GFP[1] adult Zebrafish were anesthetized and bathed in D-luciferin. After the cut of the last part of the caudal fin they were placed on a water-soaked sponge support and subjected to longitudinal *in vivo* imaging sessions. Pre-imaging acquisition was made before fin clip treatment to check the initial condition of the animals (Fig.8C). The second day after the cut, a precise light emission appears on regenerating caudal fin (Fig.8 E red arrows), it reach the highest level at the end of the first week (Fig. 8F, red arrows), and then decrease until the third week (Fig. 8G, red arrows). A week later the fish comes to the initial conditions observed before treatment (Fig.8H). These observation are in according with published data on caudal fin regeneration along with the wound healing process starts approximately 24 to 48 hours post-amputation and around 3 weeks after amputation, the caudal fin is fully restored (Poss *et al* 2003). In parallel with the signals coming from caudal fin we observed a pronounced systemic luciferase activation is evident starting from the first day (Fig.8D). In fact, light is emitted from almost all body. However, by selecting an higher threshold setting (Fig.8I), signal is clearly localized on the region of kidney and thymus (Fig.8J). Interestingly, these two organs are recognized sites for stem cell colonization and active hematopoietic regeneration in adult Zebrafish (Murayama *et al*., 2006). In fact, it is well-known in Zebrafish that thymus is colonized by neutrophilic granulocytes (Willett *et al*., 1999; Lieschke *et al*., 2001) and prothrombocytes (Lin *et al*., 2005) in 2 dpf embryos and lymphoblasts by 3 dpf (Willett *et al*., 1999). Later on, kidney produces mature myeloid and lymphoid cells starting from 2 weeks of development (Willett *et al*., 1999). During first weeks after fin clip, from the second to the twenty-first days (Fig.8E,F,G), light persists on these tissues with various proliferation waves. Four week later light is completely absent (Fig.8H). Taken together, these data demonstrate that, after fin clip, GFP and luciferase expression are induced in MITO-Luc-GFP[1] zebrafish line and strongly indicate that in this animal model it is possible to dynamically visualized induction of proliferation events in distinct body sites.

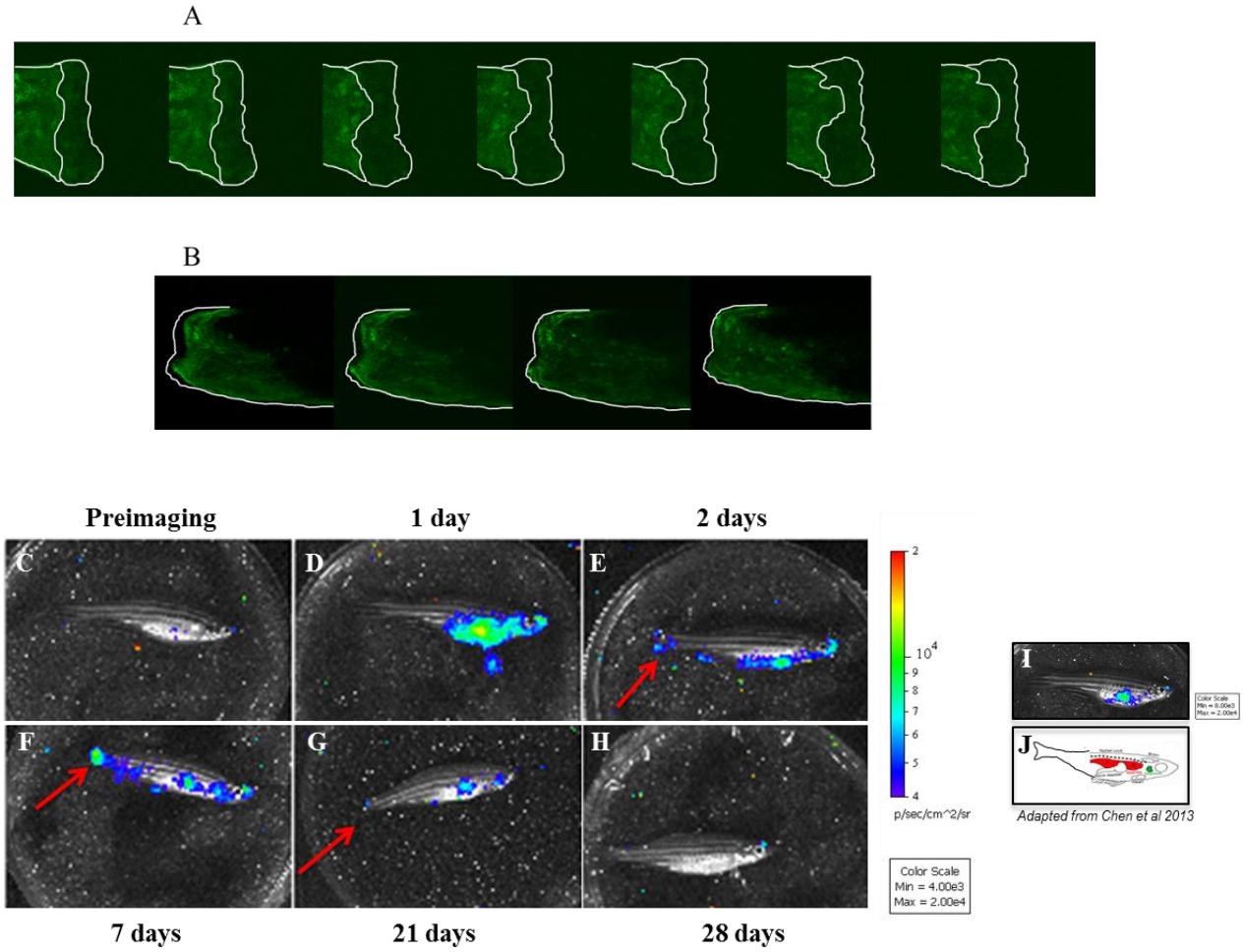

Figure 8. ***Caudal fin regeneration in MITO-Luc-GFP animals.*** Frames summarizing the GFP expression during the process of caudal fin regeneration in a 3 dpf embryos. Experiments were performed in MITO-Luc-GFP[1] **(A)** and in MITO-Luc-GFP[2] **(B).** BLI of representative MITO-Luc-GFP[1] Zebrafish before **(C)** and after 1 **(D)**, 2 **(E)**, 7 **(F)**, 21 **(G)**, 28 **(H)** days fin clip treatment. Red arrows in E, F and G indicate light coming from regenerating caudal fin. Light emitted from the animals appears in pseudocolor scaling. **(I-J)**. BLI with an higher threshold **(I)** and schematic representation of kidney and thymus, hematopoietic organs **(J)**.

Movie 3. Time laps acquisition of caudal fin regeneration in 3 dpf embryos MITO-Luc-GFP[1] after fin clip treatment. Embryo was imaged every 15 min for 14 hrs using confocal microscope.

Movie 4. Time laps acquisition of caudal fin regeneration in 3 dpf embryos MITO-Luc-GFP[2] after fin clip treatment. Embryo was imaged every 15 min for 14 hrs using confocal microscope.

5.6. Inhibition of luciferase in zebrafish embryos upon anti-proliferative treatments.

Nowadays, the residues of anti-neoplastic drugs have becoming emerging pollutants in aquatic environments, among which 5-Fluorouracil pyrimidine analog (5-FU), one of the most extensively used anti-neoplastic drugs in cancer therapy (Kovács *et al*., 2015). Recently, Zebrafish were exploited as relevant and sensitive tool to screen genotoxic potential of environmental pollutants and it has been shown that sublethal doses of 5-FU inhibit cell proliferation (Hofer *et al*., 2006).

To appreciate if could be possible to inhibit luciferase expression upon pharmacological inhibition of proliferation in MITO-Luc-GFP Zebrafish, pool of 24 hpf embryos were treated with 100mM 5FU. Pre-imaging acquisition was imaged just before treatment to check the initial condition of embryo pools upon luciferin delivery. 5FU was dissolved in water and after 5 hrs the treatment was replaced with fresh water. Successively embryos were subjected to longitudinal *in vivo* imaging sessions at sequential timing. Figure 9A shows that 18 and 24 hrs after treatment a marked inhibition of luciferase expression is evident.18 hrs later a signal increase is appreciated. Signal quantification was performed by Living Image Software (Fig.9B).

Next, embryos at 18 hpf were irradiated using X-rays at different doses. 6 hrs later, luciferase activity was measured in homogenates of untreated, 1,8 Gy treated and 2,7 Gy treated embryos groups. As shown in figure 9C, X-ray radiation determines a slight but reproducible dose dependent decrease of luciferase activity in irradiated compared with control groups. All together these results demonstrate that anti proliferative treatments induce a decrease of luciferase activity, thus strongly indicating that in this animal model it is possible to correlate the effects of anti proliferative drugs with a reduction of luciferase activity.

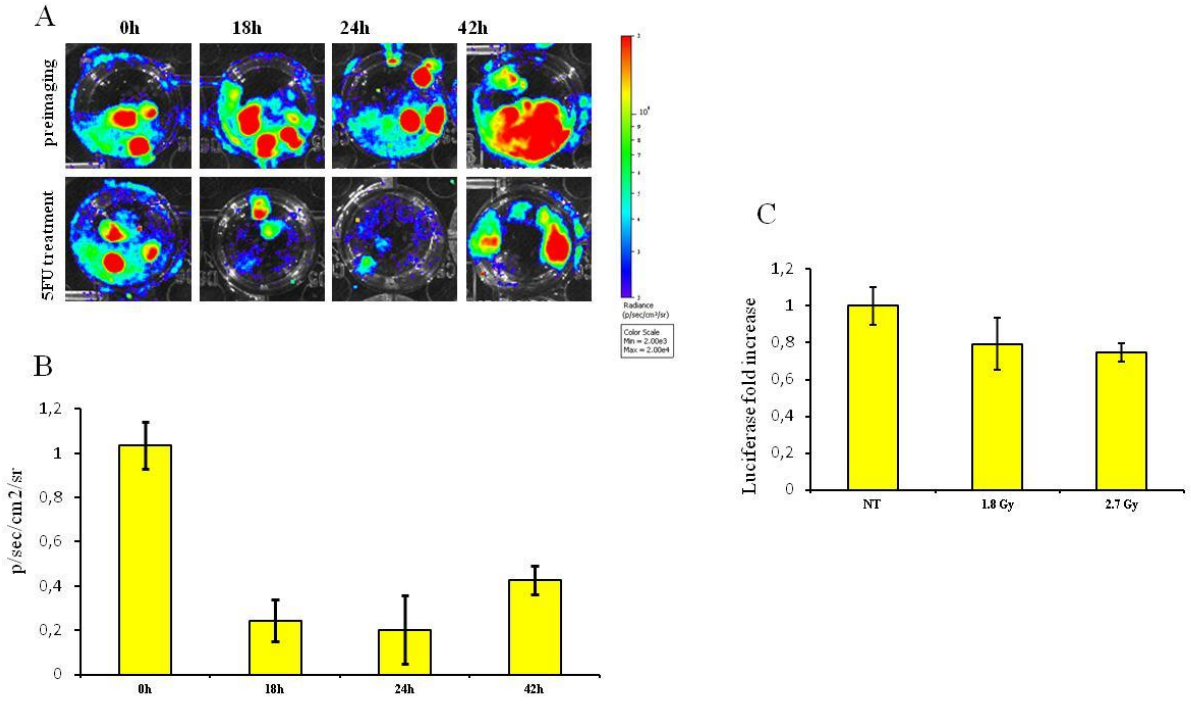

Figure 9. ***Inhibition of luciferase in zebrafish embryos upon antiproliferative treatments.*** **(A)** BLI of representative pool of MITO-Luc-GFP[1] embryos before (pre) andafter (hr 0, 18, 24) 100mM 5FU treatment. **(B)** Quantification of emitted light from each experimental timing**.** The error bars are mean standard deviations from three experiments. **(C)** Luciferase activity of pools of MITO-Luc-GFP[1] embryos 5 hrs after X-Ray treatments at indicated doses. The error bars are mean standard deviations from three experiments.

6. DISCUSSION

Despite 450 million years of evolutionary distance, cell and molecular pathways that govern signaling, proliferation, differentiation, and apoptosis are highly conserved between human and Zebrafish, thus zebrafish models represent a fundamental tool to improve treatments of malignant disease, as an intermediate experimental step between cell culture based assays and human clinical trials.

In the present study, we describe the generation and characterization of two reporter transgenic zebrafish lines in which, using the activity of a master regulator of proliferation, NF-Y, it is possible to visualize proliferation in intact animals. As a sensor of NF-Y transcriptional activity, we used a cyclinB2 promoter fragment to drive the transcription of the luciferase and GFP genes. Notably, the fact that NF-Y activity is exerted only in proliferating cells provides the unprecedented ability to follow physiological and/or pathological proliferation in every body area of these zebrafish lines. Specifically, we observed by *in vivo* and *in vitro* experiments that luciferase and GFP are mostly expressed in tissues containing proliferating cells.

This new transgenic zebrafish model, called MITO-Luc-GFP Zebrafish, is a remarkable tool not only for following NF-Y transcriptional activity *in vivo*, but also for monitoring active cell proliferation in longitudinal studies both during embryonic stage and during the entire animal life, by confocal analysis or BLI technique, respectively. So that, our versatile tool consents to choose the most appropriated method of analysis according to the experimental issue should be addressed, overcoming the major limitations and exploiting the advantages of each method. Due to the optical transparency, defective or pathological phenotypes can be analyzed in the whole-mount embryos. In this context, the use of fluorescent proteins that allows the study of the disease processes are particularly advantageous. On the other hand, the detection of fluorescent proteins in living adult animals is particularly tricky, due to the presence of the no-transparent skin of adult Zebrafish that avoids detecting signals from an internal organ and restricts the observation on tissues near the body surface. Multiple advantages of bioluminescence overcome fluorescence detection for tissue proliferation and regeneration research in living adult animals. Bioluminescence allows the visualization of signal in deep tissues in a quantitative manner. Especially, this technique eliminates the necessity of qualitative histological analysis on fixed tissues. Thus, the ability to monitor individual animals throughout longitudinal studies without sacrificing them for tissue collection should significantly reduce the number of animals required for experiments. It will also be possible to detect even subtle changes due to variation among individuals. Nevertheless bioluminescence imaging also has limitations. Signals could be varies in different animals and quantitative analyses

are most reliable when the data are compared within the same animal over time. Sometimes it is not possible to distinguish the structural differences between two nearby, discrete light sources. Moreover luciferase-based imaging is typically only a two-dimensional modality with a limited, typically 1- 3 mm spatial resolution due to photon scattering (Signore *et al*., 2010).

Cell proliferation in zebrafish embryos can be assessed by well-known conventional methods such as EdU or BrdU labeling (Laguerre *et al*. 2005); immunohistochemistry with antibodies against cell-cycle and proliferation markers as PCNA proliferating cell nuclear antigen (Machado *et al*., 2014) or pH3 (Hendzel *et al*.,1997). Also, fluorescent transgenic animals have been produced to label proliferating stem and progenitor cell populations (Kassen *et al*., 2008; Fukuhara *et al*, 2014). However, these methods do not allow assessment of cell proliferation in living animals. A proliferation-responsive regulatory promoter that remains largely stable during proliferation has been used to drive luciferase in our transgenic line, MITO-Luc-GFP. Thus, in these animals luciferase activity permits a quantitative *in vivo* bioluminescence assays of tissue proliferation.

In this model we expected to highlight changes in luciferase activity upon induction or inhibition of proliferation. We have here shown several evidences supporting this assumption. First, induction of luciferase activity occurs in MITO-Luc-GFP zebrafish tissues when proliferation is induced. As proof of principle, fin clip treatment was done to MITO-Luc-GFP adults, and bioluminescence was detected during the regeneration process. Of note, light is observed not only at the treated site (caudal fin), but also in distinct body sites possibly corresponding to kidney and thymus. Interestingly, these two organs are recognized sites for stem cell colonization and active hematopoietic regeneration in adult Zebrafish thus indicating a strong correlation between luciferase activity and proliferation processes. Although other experiments are needed to elucidate in detail which organs are the source of light, our data indicate that the use of BLI in entire organisms could also achieve information about systemic proliferation as a body response to injury. Second, anti proliferative chemical and radiation treatments induce a decrease of luciferase activity, thus strongly indicating that in this animal model changes of luciferase activity can be used as a tracer for changes in cell proliferation.

MITO-Luc-GFP Zebrafish, being a read out for proliferation events, would speed up in the future the evaluation of the efficacy of anti- or pro-proliferative drug candidates. In fact, MITO-Luc-GFP embryos would be highly suitable for *in vivo* screens taking into account the complexity of an intact organism. Effectively, as a complement to cell line screens, multicellular organism screens may reveal additional unknown compound (Murphey *et al*., 2006). In conclusion, MITO-Luc-GFP Zebrafish will be useful to readily and easily measure cell proliferation for several experimental

applications, ranging from oncology to regenerative medicine, for testing the efficacy of regenerative active drugs. Moreover, in oncological research, our model, if crossed with animal disease models will allow imaging of tumor progression and treatment response in the entire living animals.

7. MATERIALS AND METHODS

7.1. Zebrafish

Animal experiments performed in this study were conducted according to the "Guide lines for Care and Use of Experimental Animals" and the Italian law DL 116/92. Embryos (6hpf-72hpf), juveniles (3-6 months) and adult Zebrafish (1 year-2 year) were used for the experiments. Adult density was maintained at 3-4 per liter in all experiments.

7.2. Transgenic MITO-Luc-GFP zebrafish line

We used a described vector, pT2KXIGΔin, for the generation of the MITO-Luc-GFP reporter constructs using standard cloning procedures. The constructs, pT2KXIGΔin-MITO-Luc-GFP, were obtained by cloning a murine cyclinB2 promoter fragment into the BamHI and NcoI sites of the pT2KXIGΔin plasmid. This murine cyclinB2 promoter fragment spans the –266 to +46 base-pair region with respect to the transcription start site in front of a luciferase reporter and GFP reporter. The construct was flanked with Tol 2 sequences sites to permit transgenesis. Purified DNA was injected into one-cell zebrafish embryos.

7.3. DNA extractionand PCR analysis

Dechorionate embryos or fin fragments were lysate in Lysis Buffer (10mM TrisHCl [pH 8.0], 1mM EDTA, 0,3% Tween, 0,3% NP40), they were incubate for 10 min at 98°C, cooled in ice and incubate at 55°C over night with 1mg/ml Proteinase K. Samples were extracted with phenol-chloroform adding NaAc, precipitated with 100% ethanol and collected by centrifugation. DNA pellets were washed with 70% ethanol and were suspended in mQ water.

After genomic DNA extraction the positive transgenic animals were identified by PCR using the following primers:

Luciferase: oligonucleotide forward: 5′-ccggtactgttggtaaaatggaagacgcc -3'

oligonucleotide reverse: 5′-cggacatttcgaagtattccgcgtacgtg -3'

7.4. Inverse PCR

Genomic DNAs from both transgenic zebrafish lines were digested with *mboI* (BioLabs) restriction enzyme, having no recognition sites within the transgene insertion. Cleavage products were circularized using *T4 DNA ligase* (BioLabs) under condition that favor the formation of monomeric circle. After digestion, samples were hated to 65°C to inactivate restriction enzymes. Sample were precipitated with ethanol 100% adding 3M NaAC and amplificated with *Phusion*

High-Fidelit DNA Polymerase (BioLabs) using primers synthesized within the transgene in the opposite orientations to those normally employed for PCR. Primers for Inverse PCR are complementary to the opposite strand and orientated such that extension proceeds outward from the transgene. Reopen of the circularized molecules was not necessary. Nested primers were employed to further increase the specificity of PCR (Ochman *et al*., 1988).
Following primers were synthesized:

Inverse PCR: oligonucleotide forward: 5′- gagaggctgcaaatagcagg -3’
oligonucleotide reverse: 5′-gagctaggcttgacactaac -3’

Nested PCR: oligonucleotide forward: 5′- ccctcggatatcacggg -3’
oligonucleotide reverse: 5′-cgttctactgaagttaaatctgagg -3’

Multiple PCR products were obtained from the MITO-Luc-GFP[1] line. Sequencing has not given reliable results, indicating the presence of multiple transgene insertions. Single PCR product was obtained from the MITO-Luc-GFP[2] line. Sequencing has permitted to determine the nucleotides sequence of genomic DNA flanking the transgene (24:28293209-28293338), allowing the insertion localization in the first intron (15909bp) of the *prkag2a* gene in the 24th chromosome of zebrafish genome.

7.5. Relative-quantitative PCR analysis

Prior to performing the copy number assay, standard curves with serial dilutions of genomic DNA samples (6.25 ng, 12.5 ng, 25 ng, 50 ng) were generated for the transgene and the endogenous control genes. Slopes of -3,41 and -3,49 and correlation coefficients of 0.99749, and 0.99732 for the luciferase and cyclinB1 genes, respectively, were obtained, permitting the use of the $2^{-\Delta\Delta Ct}$ method for the relative copy number quantification. Evaluation of $2^{-\Delta\Delta Ct}$ indicates the fold change in copy number of the luciferase gene relative to the cyclinB1 gene used as calibrator. All samples were run in triplicate (Ballester *et al*., 2004).

7.6. Luciferase assay

Embryos were lysated in Lysis Reagent (Luciferase Assay Systems, Promega) shaking for 10 min at room temperature. Lysates were quick-freezed on dry ice and then equilibrated to room temperature. Lysates were mixed with Luciferase Assay Reagent (Luciferase Assay Systems, Promega) and the light produced were measured. The protein concentration was determined by Pierce BCA Protein Assay Kit, Thermo Scientific. The values were normalized for protein amounts.

7.7. Fluorescence Imaging

Fluorescence emission were detected using the ST2 Leica stereo microscope with the Nikon high resolution CCD camera, and analyzed with the NNS software. Movies were achieved by merging sequential time laps acquisition, employed using a Zeiss confocal microscope. Embryos were immobilized in a drop of 1% low-melting agarose containing 0.01 mg/l Tricaine and placed into confocal dishes Embryos were subjected to sequential acquisitions with different duration and frequency according to the stage of development.

7.8. Bioluminescence Imaging

For bioluminescence, transgenic Zebrafish (adult, juveniles, embryos) were given 50 mM D-Luciferin by bathing in aquarium water. Animals were allowed to swim in luciferin solution for 15 min to reach the plateau phase of bioluminescence. After rinsing in aquarium water, the fish were ready for imaging. For imaging, adult Zebrafish were placed in a low dose of tricaine (0.01 mg/ml) on a water-soaked sponge support to reduce stress. Quantification of light emission was performed in photons/second and visualized in a pseudo color scaling. Time exposure was 5 min. Light emission was detected using the IVIS Lumina II CCD camera system and analyzed with the Living Image 2.20 software package (Caliper Life Sciences).

7.9. Immunofluorescence

Samples were fixed in 4% paraformaldehyde, rinsed 3x in phosphate buffer saline (PBS), treated with 0,25% tripsin, rinsed 3x in Washing Buffer (1% Triton, 0.2% DMSO, PBS) and blocked for 1 hr using Blocking Buffer (0,1% Triton, 1% DMSO, 5% normal goat serum, PBS). Samples were incubated overnight at 4 °C with polyclonal anti-phospho-H3 antibody (1:750, Abcam); polyclonal anti-firefly luciferase antibody (1:400, Abcam) or monoclonal anti-GFP antibody (1:100 Merk Millipore). Samples were washed 5x in Washing Buffer, and blocked for 30 min using Blocking Buffer. Samples were incubated overnight at 4 °C with secondary antibody: Alexa 488(1:400); Alexa 546 (1:400). Samples were rinsed 2x in Washing Buffer. Nuclei were stained with DAPI, Sigma-Aldrich.

7.10. Immunohistochemistry

Adult Zebrafish were euthanized and fixed in 4% paraformaldehyde for 24 hrs. Samples were treated with I.E.D. Unit (Ion-Exchange Decal Unit, BioCare Medical) to decalcificate the tissues and embedded in paraffin. Serial sections were mounted on slides, deparaffinized in xylene, and rehydrated. Sections were blocked for 1 hr using Blocking Buffer (5% bovine serum albumin, 5%

fetal bovine serum, PBS) and incubated overnight at 4°C with polyclonal anti-phospho-H3 antibody (1:750, Abcam); polyclonal anti-firefly luciferase antibody (1:50, Novus Bio); monoclonal anti-GFP antibody (1:100, Merk Millipore) or monoclonal anti-PCNA antibody (1:100, Abcam). Sections were washed 3x in Washing Buffer, and processed following the manufacturer's instruction of the MACH1 Univeral HRP Kit (Biocare). The sections were stained with hematoxylin.

7.11. 5FU treatment

100Mm 5-Fluorouracil treatments on 24 hpf embryos were done in E3 water at 28.5 °C for 5 h, then the treatment was replaced with fresh E3 water. Embryos were subjected to longitudinal in vivo imaging sessions, before the onset, at the end, and 18, 24 and 42 hrs later the treatment.

7.12. X-Ray treatments

Different amount of X-Ray (1,8 Gy and 2,7 Gy) were applied on 24 hpf embryos. After 6 h embryos were prepared for the Luciferase Assay.

8. REFERENCE

- Ballester M, Casteló A, Ibáñez E, Sánchez A, Folch JM. **Real-time quantitative PCR-based system for determining transgene copy number in transgenic animals.** Biotechniques. 2004 Oct;37(4):610-3.
- Barriuso J, Nagaraju R, Hurlstone A. **Zebrafish: a new companion for translational research in oncology.** Clin Cancer Res. 2015 Mar 1;21(5):969-75.
- Bentley VL, Veinotte CJ, Corkery DP, Pinder JB, LeBlanc MA, Bedard K, Weng AP, Berman JN, Dellaire G. **Focused chemical genomics using zebrafish xenotransplantation as a pre-clinical therapeutic platform for T-cell acute lymphoblastic leukemia** Haematologica. 2015 Jan; 100(1): 70–76.
- Bhattacharya A1, Deng JM, Zhang Z, Behringer R, de Crombrugghe B, Maity SN. **The B subunit of the CCAAT box binding transcription factor complex (CBF/NF-Y) is essential for early mouse development and cell proliferation.** Cancer Res. 2003 Dec 1;63(23):8167-72.
- Bolognese F, Wasner M, Dohna CL, Gurtner A, Ronchi A, Muller H, Manni I, Mossner J, Piaggio G, Mantovani R, Engeland K. **The cyclin B2 promoter depends on NF-Y, a trimer whose CCAAT-binding activity is cell-cycle regulated.** Oncogene. 1999 Mar 11;18(10):1845-53.
- Bu L, Ma X, Tu Y, Shen B, Cheng Z. **Optical image-guided cancer therapy.** Curr Pharm Biotechnol. 2013;14(8):723-32.
- Bungartz G1, Land H, Scadden DT, Emerson SG. **NF-Y is necessary for hematopoietic stem cell proliferation and survival.** Blood. 2012 Feb 9;119(6):1380-9.
- Camus S, Quevedo C, Menéndez S, Paramonov I, Stouten PF, Janssen RA, Rueb S, He S, Snaar-Jagalska BE, Laricchia-Robbio L, Izpisua Belmonte JC. **Identification of phosphorylase kinase as a novel therapeutic target through high-throughput screening for anti-angiogenesis compounds in zebrafish**. Oncogene, 2012. 31(39): 4333-42.
- Caretti G, Motta MC, Mantovani R. **NF-Y associates with H3-H4 tetramers and octamers by multiple mechanisms.** Mol Cell Biol. 1999 Dec;19(12):8591-603.
- Carlsen H, Moskaug JØ, Fromm SH, Blomhoff R. **In vivo imaging of NF-kappa B activity.** J Immunol. 2002 Feb 1;168(3):1441-6.
- Chen CH, Durand E, Wang J, Zon LI, Poss KD. **zebraflash transgenic lines for in vivo bioluminescence imaging of stem cells and regeneration in adult zebrafish.** Development. 2013 Dec;140(24):4988-97.

- Ciana P, Raviscioni M, Mussi P, Vegeto E, Que I, Parker MG, Lowik C, Maggi A. **In vivo imaging of transcriptionally active estrogen receptors.** Nat Med. 2003 Jan;9(1):82-6.
- Ciana P, Biserni A, Tatangelo L, Tiveron C, Sciarroni AF, Ottobrini L, Maggi A. **A novel peroxisome proliferator-activated receptor responsive element-luciferase reporter mouse reveals gender specificity of peroxisome proliferator-activated receptor activity in liver.** Mol Endocrinol. 2007 Feb;21(2):388-400.
- Coleman SM, McGregor A.**A bright future for bioluminescent imaging in viral research.** Future Virol. 2015;10(2):169-183.
- Contag PR. **Bioluminescence imaging to evaluate infections and host response in vivo.** Methods Mol Biol. 2008;415:101-18.
- Corish P, Tyler-Smith C. **Attenuation of green fluorescent protein half-life in mammalian cells.** Protein Eng. 1999 Dec;12(12):1035-40.
- de Latouliere L, Manni I, Iacobini C, Pugliese G, Grazi GL, Perri P, Cappello P, Novelli F, Menini S, Piaggio G. **A bioluminescent mouse model of proliferation to highlight early stages of pancreatic cancer: A suitable tool for preclinical studies**. Ann Anat. 2015 Dec 15. pii: S0940-9602(15)00153-3.
- Detrich HW. **Fluorescent proteins in zebrafish cell and developmental biology.** Methods Cell Biol. 2008;85:219-41.
- Di Agostino S, Strano S, Emiliozzi V, Zerbini V, Mottolese M, Sacchi A, Blandino G, Piaggio G. **Gain of function of mutant p53: the mutant p53/NF-Y protein complex reveals an aberrant transcriptional mechanism of cell cycle regulation.** Cancer Cell, 2006. 10, 191–202.
- Dolfini D, Zambelli F, Pavesi G, Mantovani R. **A perspective of promoter architecture from the CCAAT box**. Cell Cycle. 2009 Dec 15;8(24):4127-37.
- Doyle TC, Burns SM, Contag CH. **In vivo bioluminescence imaging for integrated studies of infection.** Cell Microbiol. 2004 Apr;6(4):303-17.
- Farina A, Manni I, Fontemaggi G, Tiainen M, Cenciarelli C, Bellorini M, Mantovani R, Sacchi A, Piaggio G. **Down-regulation of cyclin B1 gene transcription in terminally differentiated skeletal muscle cells is associated with loss of functional CCAAT-binding NF-Y complex.** Oncogene, 1999. 18, 2818–2827.
- Feitsma H, E. Cuppen, **Zebrafish as a cancer model**. Mol Cancer Res, 2008. 6(5): p.685-94.

- Fukuhara S, Zhang J, Yuge S, Ando K, Wakayama Y, Sakaue-Sawano A, Miyawaki A, Mochizuki N. **Visualizing the cell-cycle progression of endothelial cells in zebrafish.** Dev Biol. 2014 Sep 1;393(1):10-23.
- Gatta R, Dolfini D, Mantovani R. **NF-Y joins E2Fs, p53 and other stress transcription factors at the apoptosis table.** Cell Death Dis. 2011 May 26;2:e162.
- Ghotra VP, He S, de Bont H, van der Ent W, Spaink HP, van de Water B, Snaar-Jagalska BE, Danen EH. **Automated whole animal bio-imaging assay for human cancer dissemination.** PLoS One. 2012;7(2):e31281.
- Goeman F, Manni I, Artuso S, Ramachandran B, Toietta G, Bossi G, Rando G, Cencioni C, Germoni S, Straino S, Capogrossi MC, Bacchetti S, Maggi A, Sacchi A, Ciana P, Piaggio G. **Molecular imaging of nuclear factor-Y transcriptional activity maps proliferation sites in live animals.** Mol Biol Cell. 2012 Apr;23(8):1467-74.
- Grskovic M, Chaivorapo C, Gaspar-Maia A, Li H, Ramalho-Santos M. **Systematic identification of cis-regulatory sequences active in mouse and human embryonic stem cells.** PLoS Genet. 2007 Aug;3(8):e145.
- Gurtner A, Manni I, Fuschi P, Mantovani R, Guadagni F, Sacchi A, Piaggio G, 2003. **Requirement for down-regulation of the CCAAT-binding activity of the NF-Y transcription factor during skeletal muscle differentiation.** Mol. Biol. Cell. 14, 2706–2715.
- Gurtner A, Fuschi P, Magi F, Colussi C, Gaetano C, Dobbelstein M, Sacchi A, Piaggio G. **NF-Y dependent epigenetic modifications discriminate between proliferating and postmitotic tissue**. PLoS One, 2008. 3, e2047.
- Hawes JJ, Reilly KM. **Bioluminescent approaches for measuring tumor growth in a mouse model of neurofibromatosis.** Toxicol Pathol. 2010 Jan;38(1):123-30.
- Hayashi M, Takai J, Yu L, Motohashi H, Moriguchi T, Yamamoto M. **Whole-Body In Vivo Monitoring of Inflammatory Diseases Exploiting Human Interleukin 6-Luciferase Transgenic Mice.** Mol Cell Biol. 2015 Oct;35(20):3590-601.
- Heasman J. **Morpholinooligos: making sense of antisense?** Dev Biol. 2002 Mar 15;243(2):209-14.
- Heilmann S, Ratnakumar K, Langdon E, Kansler E, Kim I, Campbell NR, Perry E, McMahon A, Kaufman C, van Rooijen E, Lee W, Iacobuzio-Donahue C, Hynes R, Zon L, Xavier J, White RM. **A quantitative system for studying metastasis using transparent zebrafish.** Cancer Res. 2015 Aug 17: canres.3319.2014.

- Hendzel M.J, WeiY, Mancini MA, Van HA, Ranalli T, Brinkley BR, Bazett- Jones DP, Allis CD. **Mitosis-specific phosphorylation of histone H3 initiates primarily within pericentromeric heterochromatin during G2 and spreads in an ordered fashion coincident with mitotic chromosome condensation**. Chromosoma 1997. 106,348–360.
- Hofer M, Pospísil M, Vacek A, Holá J, Znojil V, Weiterová L, Streitová D. **Effects of adenosine A(3) receptor agonist on bone marrow granulocytic system in 5-fluorouracil-treated mice.** Eur J Pharmacol. 2006 May 24;538(1-3):163-7.
- Huang P, Zhu Z, Lin S, Zhang B. **Reverse genetic approaches in zebrafish**. J Genet Genomics, 2012. 39(9)
- Hutchens M, Luker GD. **Applications of bioluminescence imaging to the study of infectious diseases.** Cell Microbiol. 2007 Oct;9(10):2315-22.
- Ishikawa TO, Jain NK, Taketo MM, Herschman HR. **Imaging cyclooxygenase-2 (Cox-2) gene expression in living animals with a luciferase knock-in reporter gene.** Mol Imaging Biol. 2006 May-Jun;8(3):171-87.
- Ivanova AS, Shandarin IN, Ermakova GV, Minin AA, Tereshina MB, Zaraisky AG. **The secreted factor Ag1 missing in higher vertebrates regulates fins regeneration in Danio rerio.** Sci Rep. 2015 Jan 29;5:8123.
- Ju B, Chen W, Orr BA, Spitsbergen JM, Jia S, Eden CJ, Henson HE, Taylor MR. **Oncogenic KRAS promotes malignant brain tumors in zebrafish.** Mol Cancer. 2015 Feb 3;14:18.
- Ju HL, Calvisi DF, Moon H, Baek S, Ribback S, Dombrowski F, Cho KJ, Chung SI , Han KH, Ro SW. **Transgenic mouse model expressing P53(R172H), luciferase, EGFP, and KRAS(G12D) in a single open reading frame for live imaging of tumor**. Sci Rep.2015 Jan 27;5:8053.
- Kamei K, Ishikawa TO, Herschman HR. **Transgenic mouse for conditional, tissue-specific Cox-2 overexpression.** Genesis. 2006 Apr;44(4):177-82.
- Kassen SC, Thummel R, Burket CT, Campochiaro LA, Harding MJ, Hyde DR. **The Tg(ccnb1:EGFP) transgenic zebrafish line labels proliferating cells during retinal development and regeneration.** Mol Vis. 2008 May 19;14:951-63.
- Keller AF1, Gravel M, Kriz J. **Live imaging of amyotrophic lateral sclerosis pathogenesis: disease onset is characterized by marked induction of GFAP in Schwann cells.** Glia. 2009 Aug 1;57(10):1130-42.
- Kimmel CB, Ballard WW, Kimmel SR, Ullmann B, Schilling TF: **Stages of embryonic development of the zebrafish**. Dev Dyn 1995, 203:253-310.

- Kovács R1, Bakos K, Urbányi B, Kövesi J, Gazsi G, Csepeli A, Appl ÁJ, Bencsik D, Csenki Z, Horváth Á. **Acute and sub-chronic toxicity of four cytostatic drugs in zebrafish.** Environ Sci Pollut Res Int. 2015 Jul 24.
- Kuroyanagi M, Katayama T, Imai T, Yamamoto Y, Chisada S, Yoshiura Y, Ushijima T, Matsushita T, Fujita M, Nozawa A, Suzuki Y, Kikuchi K1, Okamoto H. **New approach for fish breeding by chemical mutagenesis: establishment of TILLING method in fugu (Takifugu rubripes) with ENU mutagenesis**. BMC Genomics, 2013. 14:786.
- Laguerre L, Soubiran F, Ghysen A, König N, Dambly-Chaudière C. **Cell proliferation in the developing lateral line system of zebrafish embryos.** Dev Dyn. 2005 Jun;233(2):466-72.
- Law GH, Gandelman OA, Tisi LC, Lowe CR, Murray JA. **Mutagenesis of solvent-exposed amino acids in Photinus pyralis luciferase improves thermostability and pH-tolerance.** Biochem J. 2006 Jul 15;397(2):305-12.
- Lieschke GJ, Oates AC, Crowhurst MO, Ward AC, Layton JE. **Morphologic and functional characterization of granulocytes and macrophages in embryonic and adult zebrafish.** Blood. 2001 Nov 15;98(10):3087-96.
- Lin HF, Traver D, Zhu H, Dooley K, Paw BH, Zon LI, Handin RI. **Analysis of thrombocyte development in CD41-GFP transgenic zebrafish.** Blood. 2005 Dec 1;106(12):3803-10.
- Lipshutz GS, Gruber CA, Cao Y, Hardy J, Contag CH, Gaensler KM. **In utero delivery of adeno-associated viral vectors: intraperitoneal gene transfer produces long-term expression.** Mol Ther. 2001 Mar;3(3):284-92.
- Lu JW, Ho YJ, Yang YJ, Liao HA, Ciou SC, Lin LI, Ou DL. **Zebrafish as a disease model for studying human hepatocellular carcinoma.** World J Gastroenterol. 2015 Nov 14;21(42):12042-58.
- Luker GD, Luker KE. **Optical imaging: current applications and future directions.** J Nucl Med. 2008 Jan;49(1):1-4.
- Luker KE, Hutchens M, Schultz T, Pekosz A, Luker GD. **Bioluminescence imaging of vaccinia virus: effects of interferon on viral replication and spread.** Virology. 2005 Oct 25;341(2):284-300.
- Luo J, Ho P, Steinman L, Wyss-Coray T. **Bioluminescence in vivo imaging of autoimmune encephalomyelitis predicts disease.** J Neuroinflammation. 2008 Feb 1;5:6.

- Machado SP, Cunha V, Reis-Henriques MA, Ferreira M. **Histopathological lesions, P-glycoprotein and PCNA expression in zebrafish (Danio rerio) liver after a single exposure to diethylnitrosamine.** Environ Toxicol Pharmacol. 2014 Nov;38(3):720-32.
- Manni I, Caretti, G., Artuso, S., Gurtner, A., Emiliozzi, V., Sacchi, A., Mantovani, R., Piaggio, G. **Posttranslational regulation of NF-YA modulates NF-Y transcriptional activity**. Mol. Biol.Cell, 2008. 19, 5203–5213.
- Mirbahai L, Williams TD, Zhan H, Gong Z, Chipman JK. **Comprehensive profiling of zebrafish hepatic proximal promoter CpG island methylation and its modification during chemical carcinogenesis.** BMC Genomics. 2011 Jan 4;12:3.
- Momota H, Holland EC. **Bioluminescence technology for imaging cell proliferation.** Curr Opin Biotechnol. 2005 Dec;16(6):681-6.
- Murayama E, Kissa K, Zapata A, Mordelet E, Briolat V, Lin H F, Handin R I and Herbomel P. **Tracing hematopoietic precursor migration to successive hematopoietic organs during zebrafish development.** Immunity 2006. 25, 963- 975.
- Murphey RD, Stern HM, Straub CT, Zon LI. **A chemical genetic screen for cell cycle inhibitors in zebrafish embryos.** Chem Biol Drug Des. 2006 Oct;68(4):213-9.
- Niethammer P, Grabher C, Look AT, Mitchison TJ. **A tissue-scale gradient of hydrogen peroxide mediates rapid wound detection in zebrafish.** Nature. 2009 Jun 18;459 (7249):996-9.
- Notebaert S, Carlsen H, Janssen D, Vandenabeele P, Blomhoff R, Meyer E. **In vivo imaging of NF-kappaB activity during Escherichia coli-induced mammary gland infection.** Cell Microbiol. 2008 Jun;10(6):1249-58.
- Ochman H1, Gerber AS, Hartl DL. **Genetic applications of an inverse polymerase chain reaction.** Genetics. 1988 Nov;120(3):621-3.
- O'Neill K, Lyons SK, Gallagher WM, Curran KM, Byrne AT. **Bioluminescent imaging: a critical tool in pre-clinical oncology research.** J Pathol. 2010 Feb;220(3):317-27.
- Peterson RT, Link BA, Dowling JE, Schreiber S. **Small molecule developmental screens reveal the logic and timing of vertebrate development.** Proc Natl Acad Sci USA 2000, 97:12965-12969.
- Rizzi N, Manni I, Vantaggiato C, Delledonne GA, Gentileschi MP, Maggi A, Piaggio G, Ciana P. **In vivo imaging of cell proliferation for a dynamic, whole body, analysis of undesired drug effects**.Toxicol Sci. 2015 Jun;145(2):296-306.
- Rocchetta HL, Boylan CJ, Foley JW, Iversen PW, LeTourneau DL, McMillian CL, Contag PR, Jenkins DE, Parr TR Jr. **Validation of a noninvasive, real-time imaging technology**

using bioluminescent Escherichia coli in the neutropenic mouse thigh model of infection. Antimicrob Agents Chemother. 2001 Jan;45(1):129-37.

- Sadikot RT, Zeng H, Joo M, Everhart MB, Sherrill TP, Li B, Cheng DS, Yull FE, Christman JW, Blackwell TS. **Targeted immunomodulation of the NF-kappaB pathway in airway epithelium impacts host defense against Pseudomonas aeruginosa.** J Immunol. 2006 Apr 15;176(8):4923-30.
- Santoriello C and Zon LI, **Hooked! Modeling human disease in zebrafish**. J Clin Invest, 2012. 122(7): p. 2337-43.
- Sato A, Klaunberg B, Tolwani R. **In vivo bioluminescence imaging.** Comp Med. 2004 Dec;54(6):631-4.
- Sciortino S, Gurtner A, Manni I, Fontemaggi G, Dey A, Sacchi A, Ozato K, Piaggio G, 2001. **The cyclin B1 gene is actively transcribed during mitosis in HeLa cells**. EMBO. Rep 2, 1018–1023.
- Shah AN, Davey CF, Whitebirch AC, Miller AC, Moens CB. **Rapid reverse genetic screening using CRISPR in zebrafish.** Nat Methods. 2015 Jun;12(6):535-40.
- Sharma PK, Engels E, Van Oeveren W, Ploeg RJ, van Henny der Mei C, Busscher HJ, Van Dam GM, Rakhorst G. **Spatiotemporal progression of localized bacterial peritonitis before and after open abdomen lavage monitored by in vivo bioluminescent imaging.** Surgery. 2010 Jan;147(1):89-97.
- Signore A, Mather SJ, Piaggio G, Malviya G, Dierckx RA. **Molecular imaging of inflammation/infection: nuclear medicine and optical imaging agents and methods.** Chem Rev. 2010 May 12;110(5):3112-45.
- Spitsbergen J, **Imaging neoplasia in Zebrafish**. Nat Methods, 2007. 4(7): p. 548-9
- Sydow A, Hochgräfe K, Könen S, Cadinu D, Matenia D, Petrova O, Joseph M, Dennissen FJ, Mandelkow EM. **Age-dependent neuroinflammation and cognitive decline in a novel Ala152Thr-Tau transgenic mouse model of PSP and AD**. ActaNeuropatholCommun. 2016 Feb 25;4(1):17.
- Taylor KL, Grant NJ, Temperley ND, Patton EE. **Small molecule screening in zebrafish: an in vivo approach to identifying new chemical tools and drug leads.** Cell Commun Signal. 2010 Jun 12;8:11.
- Thompson SM, Callstrom MR, Knudsen BE, Anderson JL, Sutor SL, Butters KA, Kuo C, Grande JP, Roberts LR, Woodrum DA. **Molecular bioluminescence imaging as a noninvasive tool for monitoring tumor growth and therapeutic response to MRI-**

guided laser ablation in a rat model of hepatocellular carcinoma. InvestRadiol. 2013;48(6):413-21.

- Veinotte CJ, Dellaire G, Berman JN. **Hooking the big one: the potential of zebrafish xenotransplantation to reform cancer drug screening in the genomic era.** Dis Model Mech. 2014 Jul;7(7):745-54.
- White RM, Sessa A, Burke C, Bowman T, LeBlanc J, Ceol C, Bourque C, Dovey M, Goessling W, Burns CE, Zon LI. **Transparent adult zebrafish as a tool for in vivo transplantation analysis.** Cell Stem Cell. 2008 Feb 7;2(2):183-9.
- Willett CE, Cortes A, Zuasti A, Zapata AG. **Early hematopoiesis and developing lymphoid organs in the zebrafish.** Dev Dyn. 1999 Apr;214(4):323-36.
- Zangani M, Carlsen H, Kielland A, Os A, Hauglin H, Blomhoff R, Munthe LA, Bogen B. **Tracking early autoimmune disease by bioluminescent imaging of NF-kappaB activation reveals pathology in multiple organ systems.** Am J Pathol. 2009 Apr;174(4):1358-67.
- Zhang N, Ahsan MH, Purchio AF, West DB. **Serum amyloid A-luciferase transgenic mice: response to sepsis, acute arthritis, and contact hypersensitivity and the effects of proteasome inhibition.** J Immunol. 2005 Jun 15;174(12):8125-34.
- Zhang N, Weber A, Li B, Lyons R, Contag PR, Purchio AF, West DB. **An inducible nitric oxide synthase-luciferase reporter system for in vivo testing of anti-inflammatory compounds in transgenic mice.** J Immunol. 2003 Jun 15;170(12):6307-19.
- Zhao H1, Tang C, Cui K, Ang BT, Wong ST. **A screening platform for glioma growth and invasion using bioluminescence imaging. Laboratory investigation**. J Neurosurg. 2009 Aug;111(2):238-46.
- Zhao S, Huang J, Ye J. **A fresh look at zebrafish from the perspective of cancer research.** J Exp Clin Cancer Res. 2015 Aug 12;34:80.

G Model
AANAT-51000; No. of Pages 7
ARTICLE IN PRESS

Annals of Anatomy xxx (2015) xxx–xxx

Contents lists available at ScienceDirect

Annals of Anatomy

journal homepage: www.elsevier.com/locate/aanat

A bioluminescent mouse model of proliferation to highlight early stages of pancreatic cancer: A suitable tool for preclinical studies

Luisa de Latouliere[a], Isabella Manni[a,**], Carla Iacobini[b], Giuseppe Pugliese[b], Gian Luca Grazi[c], Pasquale Perri[c], Paola Cappello[d,e], Franco Novelli[d,e], Stefano Menini[b], Giulia Piaggio[a,*]

[a] Department of Research, Advanced Diagnostics and Technological Innovation, Regina Elena National Cancer Institute, Via Elio Chianesi 53, Rome 00144, Italy
[b] Department of Clinical and Molecular Medicine, Sapienza University of Rome, Via di Grottarossa 1035-1039, Rome 00189, Italy
[c] Department of Experimental Oncology, Regina Elena National Cancer Institute, Via Elio Chianesi 53, Rome 00144, Italy
[d] Department of Molecular Biotechnologies and Health Sciences, University of Turin, Via Nizza 52, Torino 10126, Italy
[e] Center for Experimental Research and Medical Studies, Città della Salute e della Scienza di Torino, Via Santena 5, Torino 10126, Italy

ARTICLE INFO

Article history:
Received 16 October 2015
Received in revised form
16 November 2015
Accepted 17 November 2015
Available online xxx

Keywords:
Pancreatic cancer
Disease animal models
Comparative pathology
Molecular imaging
Proliferation

SUMMARY

Transgenic mouse models designed to recapitulate genetic and pathologic aspects of cancer are useful to study early stages of disease as well as its progression. Among several, two of the most sophisticated models for pancreatic ductal adenocarcinoma (PDAC) are the *LSL-Kras$^{G12D/+}$;Pdx-1-Cre* (KC) and *LSL-Kras$^{G12D/+}$;LSL-Trp53$^{R172H/+}$;Pdx-1-Cre* (KPC) mice, in which the Cre-recombinase regulated by a pancreas-specific promoter activates the expression of oncogenic *Kras* alone or in combination with a mutant *p53*, respectively. Non-invasive *in vivo* imaging offers a novel approach to preclinical studies introducing the possibility to investigate biological events in the *spatio*/temporal dimension. We recently developed a mouse model, *MITO-Luc*, engineered to express the luciferase reporter gene in cells undergoing active proliferation. In this model, proliferation events can be visualized non-invasively by bioluminescence imaging (BLI) in every body district *in vivo*. Here, we describe the development and characterization of *MITO-Luc*-KC- and -KPC mice. In these mice we have now the opportunity to follow PDAC evolution in the living animal in a time frame process. Moreover, by relating *in vivo* and *ex vivo* BLI and histopathological data we provide evidence that these mice could represents a suitable tool for pancreatic cancer preclinical studies. Our data also suggest that aberrant proliferation events take place early in pancreatic carcinogenesis, before tumour appearance.

1. Introduction

Pancreatic ductal adenocarcinoma (PDAC) is incurable with patients often presenting with metastatic disease resistant to therapy. The disease progresses through pancreatic intraepithelial neoplasia (PanIN) lesions to PDAC. Histologically, PanINs are divided into four stages, PanIN-1A, PanIN-1B, PanIN-2 and PanIN-3, defined by increasing degrees of cellular architectural atypia. PDAC is further characterized by a massive stromal reaction and inflammation. Genetically, activating mutations in *Kras* gene seem to be an ubiquitous event, although mutations in *p53* or other genes are also common (Hidalgo, 2012). Early detection is the key to improving survival in PDAC. However several factors contribute to make diagnosis of pancreatic cancer difficult at early stages: the anatomical location of the pancreas, the symptoms that are typically associated with advanced disease and the low resolution of conventional imaging modalities. Thus, early detection strategies of sporadic pancreatic cancer are urgently needed.

Genetically engineered mouse models (GEMMs) of cognate human diseases allow the identification of molecular mechanisms of disease pathogenesis (Tuveson and Hanahan, 2011). Several GEMMs that accurately mimic the pathophysiological features of human PDAC have been described (Tuveson and Hingorani, 2005; Cappello and Novelli, 2013). In particular, a mouse model (KC), in which a "*lox–stop–lox*" *Kras^{G12D}* allele is expressed in murine pancreatic progenitor cells using a pancreas-specific Cre recombinase

Abbreviations: PDAC, pancreatic ductal adenocarcinoma; KC, *LSL-Kras$^{G12D/+}$, Pdx-1-Cre*; KPC, *LSL-Kras$^{G12D/+}$, LSL-Trp53$^{R172H/+}$, Pdx-1-Cre*; PanIN, pancreatic intraepithelial neoplasia; BLI, bioluminescence imaging.

* Corresponding author. Tel.:+39 06 5266 2458; fax: +39 06 4180 526.
** Corresponding author. Tel.:+39 06 5266 2585; fax: +39 06 4180 526.
E-mail addresses: manni@ifo.it (I. Manni), piaggio@ifo.it (G. Piaggio).

http://dx.doi.org/10.1016/j.aanat.2015.11.010
0940-9602/

Please cite this article in press as: de Latouliere, L., et al., A bioluminescent mouse model of proliferation to highlight early stages of pancreatic cancer: A suitable tool for preclinical studies. Ann. Anatomy (2015), http://dx.doi.org/10.1016/j.aanat.2015.11.010

and that recapitulates all human features developing both preneoplastic and invasive PDAC, has been characterized (Hingorani et al., 2003). Moreover, in a mouse model that incorporates a *p53* mutation corresponding to the $Trp53^{R172H}$ hotspot mutation in human cancers (KPC), it has been demonstrated that the expression of an endogenous $Kras^{G12D}$ allele cooperates with that of a concomitant *p53* mutation to closely recapitulate the human disease at the pathophysiological and molecular level showing accelerated disease onset and metastasis (Hingorani et al., 2005). Although these models have been useful for therapeutic vaccination and pharmacological treatment in several preclinical studies (Cappello et al., 2013; Cappello and Novelli, 2013; Capello et al., 2013), the current methodological approaches are static and restrict the analysis to a specific phase of tumourigenesis or to a particular snapshot of time, therefore, they do not provide a dynamic view of carcinogenesis useful to identify early steps for which the environment is compulsory for tumour progression.

Non-invasive bioluminescence imaging (BLI) is a powerful tool for studying molecular events over time in a living organism (Signore et al., 2010). When combined with cancer models, this technology offers an unprecedented opportunity to investigate molecular events resulting in neoplastic development and progression in the entire organism. We have recently developed a reporter mouse model, the *rep*TOP™ *mito*IRE (*MITO-Luc*), in which it is possible to measure physiological and/or aberrant proliferation in any body tissue by BLI (Goeman et al., 2012; Spallotta et al., 2013; Oliva et al., 2013; Rizzi et al., 2015). In these mice, the transcription of the firefly luciferase reporter gene is selectively induced during the cell cycle by the transcription factor NF-Y, a trimeric transcription activator composed of NF-YA, NF-YB, and NF-YC subunits, all required for DNA binding. The NF-Y complex exerts its activity only in proliferating cells regulating basal transcription of regulatory genes responsible for cell cycle progression (Farina et al., 1999; Manni et al., 2001; Sciortino et al., 2001; Gurtner et al., 2003, 2008, 2010; Di Agostino et al., 2006; Manni et al., 2008).

Deregulation of cell cycle and consequent aberrant proliferation have been implicated in the early steps of the carcinogenic process, including PDAC (Hezel et al., 2006). Thus, we hypothesized that the visualization of hyperproliferation occurring during early carcinogenesis could allow us to identify the first stages of tumour development. Based on this hypothesis we crossed KC and KPC mice, in which the somatic activation of $Kras^{G12D}$ (KC) and mutant $Trp53^{R172H}$ (KPC) is mediated by *Pdx-1-Cre* (Hingorani et al., 2003, 2005), with *MITO-Luc* mice (Goeman et al., 2012) generating MKC and MKPC mouse models. By correlating BLI and histopathological analysis of the pancreas from these mice we provide evidence that we are able to follow tumour evolution in terms of cell proliferation in a time frame manner. Of note, we have identified early steps of pancreatic carcinogenesis thus making these models useful for preclinical pharmacological studies.

2. Material and methods

2.1. Mouse strains

All animal studies were approved by the Institutional Animal Care of the Regina Elena National Cancer Institute and by the Government Committee of National Minister of Health and were conducted according with EU Directive 2010/63/EU for animal experiments http://ec.europa.eu/environment/chemicals/lab_animals/legislation_en.htm $LSL\text{-}Kras^{G12D/+}$;$LSL\text{-}Trp53^{R172H/+}$ mice and *Pdx-1-Cre* transgenic mice (Hingorani et al., 2003, 2005) were interbred with *MITO-Luc* reporter mice (Goeman et al., 2012) to obtain *MITO*;$LSL\text{-}Kras^{G12D/+}$;*Pdx-1-Cre* and *MITO*;$LSL\text{-}Kras^{G12D/+}$;$LSL\text{-}Trp53^{R172H/+}$;*Pdx-1-Cre*, respectively. The $LSL\text{-}Kras^{G12D/+}$ and $LSL\text{-}Trp53^{R172H/+}$ lineages were maintained in the heterozygous state.

2.2. Genotyping of transgenic mice

After genomic DNA extraction of tail biopsies, the positive founder animals were identified by PCR using the following primers specific for the transgenes:

MITO:	oligonucleotide up:	5′-TGTAGACAAGGAAACAACAAA-GCCTGGTGGCC;
	oligonucleotide down:	5′-GGCGTCTTCCATTTTACCAACAG-TACCGG.
Kras:	oligonucleotide 1:	5′-GTCTTTCCCCAGCACAGTGC;
	oligonucleotide 2:	5′-CTCTTGCCTACGCCACCAGCTC;
	oligonucleotide 3	5′-AGCTAGCCACCATGGCTTGAGT-AAGTCTGCA.
Trp53:	oligonucleotide 1:	5′-AGCTAGCCACCATGGCTTGAGT-AAGTCTGCA;
	oligonucleotide 2:	5′-TTACACATCCAGCCTCTGTGG;
	oligonucleotide 3:	5′-CTTGGAGACATAGCCACACTG.
Pdx-1-Cre:	oligonucleotide up:	5′-ATGCTTCTGTCCGTTTGCCG;
	oligonucleotide down:	5′-TGAGTGAACGAACCTGGTCG.

2.3. Histology

Tissues were fixed in 10% neutral buffered formalin (Sigma) for 24 h, dehydrated through a graded series of ethyl alcoho solutions and paraffin embedded. Pancreatic tissue was cut into 5-μm sections and stained with haematoxylin and eosin (H&E) for morphological assessment. Four non serial pancreatic sections were examined and images were acquired using a Nikon Eclipse E600 light microscope equipped with Olympus C-3030 digita camera.

2.4. In vivo *and* ex vivo *BLI*

For *in vivo* BLI, mice were anesthetized and 75 mg/kg of D-luciferin (Caliper, PerkinElmer company) was injected intraperitoneally. Ten minutes later, quantification of light emission was acquired for 5 min. Signal was detected using the IVIS Lumina II CCD camera system and analysed with the Living Image 2.20 software package (Caliper Life Sciences). Photon emission was measured in specific regions of interest (ROIs). Data were expressed as photon/second/cm^2/steradiant (p/s/cm^2/sr). The intensity of bioluminescence was colour-coded for imaging purposes; the scale used in each experiment is reported in each figure. For *ex vivo* BLI experiments, animals were sacrificed after *in vivo* BLI sessions and immediately subjected to a BLI session. Images of organs were detected as for the live animals.

3. Results and discussion

3.1. Generation of bioluminescent PDAC mouse models

A mouse model has been previously described in which the expression of $Trp53^{R172H}$, concomitantly with that of $Kras^{G12D}$, leads to the development of invasive and metastatic PDAC that recapitulates clinical, histopathological, and genomic features of the cognate human disease (Hingorani et al., 2005). In order to visualize proliferation events during pancreatic tumour evolution we crossed these mice with the *MITO-Luc* mice that we recently described as a useful tool for tracking proliferation events *in vivo* in longitudinal studies in any body region. To this end, we first

Please cite this article in press as: de Latouliere, L., et al., A bioluminescent mouse model of proliferation to highlight early stages of pancreatic cancer: A suitable tool for preclinical studies. Ann. Anatomy (2015), http://dx.doi.org/10.1016/j.aanat.2015.11.010

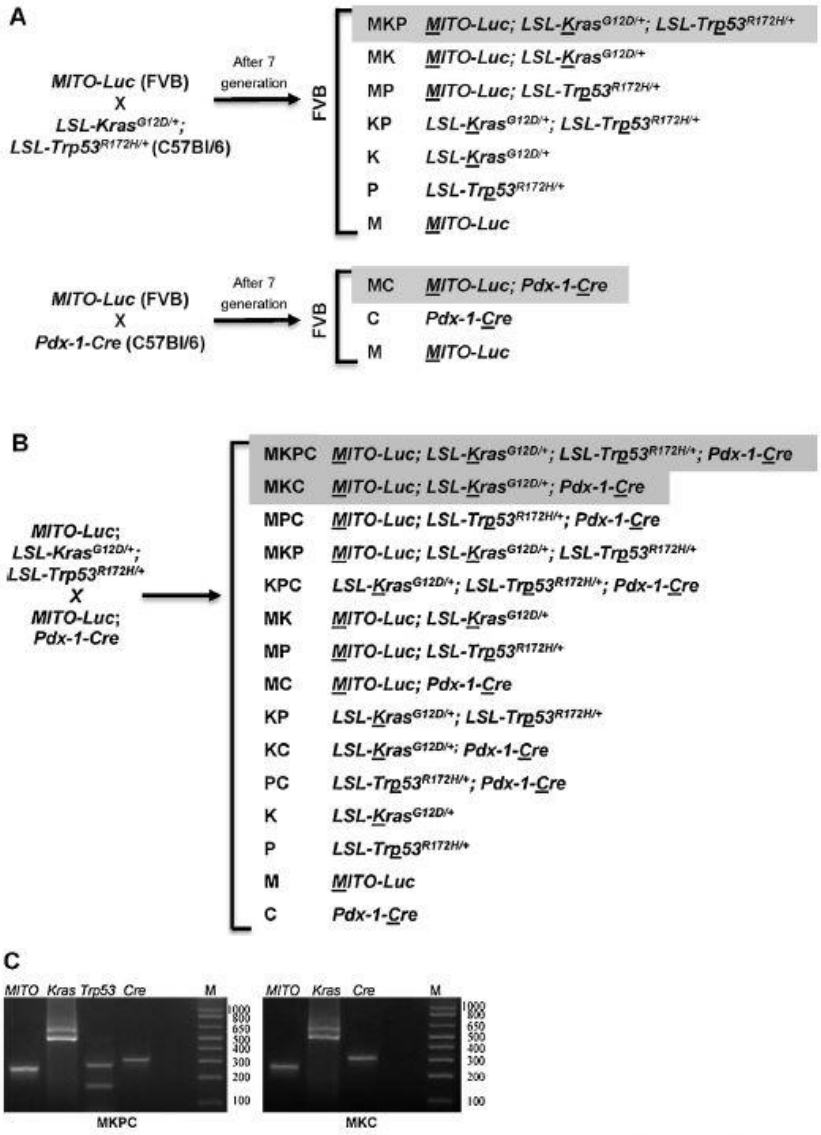

Fig. 1. *Genetic strategy for generation of bioluminescent pancreatic ductal adenocarcinoma mouse models.* (A): Schematic representation of different genotype transgenic mice obtained from *MITO-Luc* mice (FVB background) crossed with *LSL-Kras$^{G12D/+}$;LSL-Trp53$^{R172H/+}$* mice (C57Bl/6 background) and *MITO-Luc* mice (FVB background) crossed with with *Pdx-1-Cre* mice (C57Bl/6 background). To obtain a pure genetic background, mice were backcrossed into the FVB background for more than seven generations. The genotypes used for the crossing in B are indicated in gray. (B) Schematic representation of different genotype transgenic mice obtained from *MITO-Luc;LSL-Kras$^{G12D/+}$;LSL-Trp53$^{R172H/+}$* mice crossed with *MITO-Luc;Pdx-1-Cre* mice. In gray, genotypes used in the experiments described in this paper. (C) PCR of tail DNA from 1-month-old mice, *MITO-Luc;LSL-Kras$^{G12D/+}$;LSL-Trp$^{H172R/+}$;Pdx-1-Cre* and *MITO-Luc;LSL-KRAS$^{G12D/+}$;Pdx-1-Cre* mice. The bands represent the presence of the indicated cassettes. PCR products were separated on a 2% agarose gel. Molecular weight markers (1Kb Plus DNA Ladder, Invitrogen) was in the last lane from left.

crossed *MITO-Luc* mice (FVB background) with *LSL-Kras$^{G12D/+}$;LSL-Trp53$^{R172H/+}$* mice and with *Pdx-1-Cre* transgenic mice (C57Bl/6 background), respectively (Hingorani et al., 2005). To have a pure genetic background the mice were backcrossed into the FVB background for more than seven generations (Fig. 1A). Next, the *MITO-Luc;LSL-Kras$^{G12D/+}$;LSL-Trp53$^{R172H/+}$* genotype has been interbred with *MITO-Luc;Pdx-1-Cre* transgenic mice. Among the different genotypes depicted in Fig. 1B we focused our attention on *MITO-Luc;LSL-Kras$^{G12D/+}$;LSL-Trp53$^{R172H/+}$;Pdx-1-Cre* (MKPC) and *MITO-Luc;LSL-Kras$^{G12D/+}$;Pdx-1-Cre* (MKC). By specific PCR, the presence of the transgenes was assessed in the tail DNA (Fig. 1C).

3.2. PDAC frequency and histological features of pre-invasive and invasive pancreatic lesions in FVB-based mouse models

In MKPC mice in the FVB strain the prevalence of PDAC was 58.3% at 16 weeks of age and earliest tumour onset was histologically documented at 6 weeks of age, while in MKC mice the prevalence of PDAC was 16.6% at 16 weeks of age and earliest tumour onset was histologically documented at 11 weeks of age. Thus, MKPC mice have a reduced tumour-free survival, which is consistent with the reduced lifespan of KPC compared with KC mice described in the literature (median survival time of 203 for KPC *vs* 336 days for KC mice) (Hingorani et al., 2005; Cappello et al., 2013).

Please cite this article in press as: de Latouliere, L., et al., A bioluminescent mouse model of proliferation to highlight early stages of pancreatic cancer: A suitable tool for preclinical studies. Ann. Anatomy (2015), http://dx.doi.org/10.1016/j.aanat.2015.11.010

Table 1
PDAC prevalence in MKPC, MKC and MC mice at 6, 11 and 16 weeks of age. MKPC = *MITO-Luc;LSL-Kras$^{G12D/+}$;LSL-Trp53$^{R172H/+}$;Pdx-1-Cre*; MKC = *MITO-Luc;LSL-Kras$^{G12D/+}$;Pdx-1-Cre*; MC = *MITO-Luc;Pdx-1-Cre*; PanINs = pancreatic intraepithelial neoplasia; PDAC = pancreatic ductal adenocarcinoma; n.d. = not detected.

Genotype	PDAC 6Week	PDAC 11Week	PDAC 16Week	% PDAC 6Week	% PDAC 11Week	% PDAC 16Week	earliest tumor of uptake
MPKC	2/24	5/16	7/12	8.33	31.25	58.33	6Week
MKC	0/21	1/21	2/12	0	4.76	16.66	11Week
MC	0/17	0/14	0/9	0	0	0	–

Of note, none of the *MITO-Luc; Pdx-1-Cre* (MC) control mice developed tumours (Table 1). From a morphological point of view, MKPC and MKC mice developed pre-invasive and invasive ductal pancreatic cancer with the same histological features as those described for KPC and KC mice (Hingorani et al., 2003, 2005). In particular, the pancreas of MKPC and MKC mice developed PanIN lesions with complete penetrance. In fact, these ductal lesions were recognized in all the MKPC and MKC mice analysed, with or without an associated PDAC. Finally, PDAC developed in both MKPC and MKC mice showed a variable degree of differentiation, from well differentiated to undifferentiated. Representative examples of the invasive ductal adenocarcinoma seen in these animals are shown in Fig. 2 (panels A–J). In contrast, no pre-invasive or invasive ductal lesions were observed in pancreas from age-matched control mice (MC) (Fig. 2, panel K).

Taken together the *MITO-Luc* transgenic cassette does not influence the PDAC development already described in KPC and KC mouse models (Hingorani et al., 2005).

3.3. Longitudinal monitoring of PDAC-associated proliferation by in vivo and ex vivo BLI and its correlation with histopathology

Next, we asked whether bioluminescent emission associated with tissue proliferation could be useful to identify early and/or

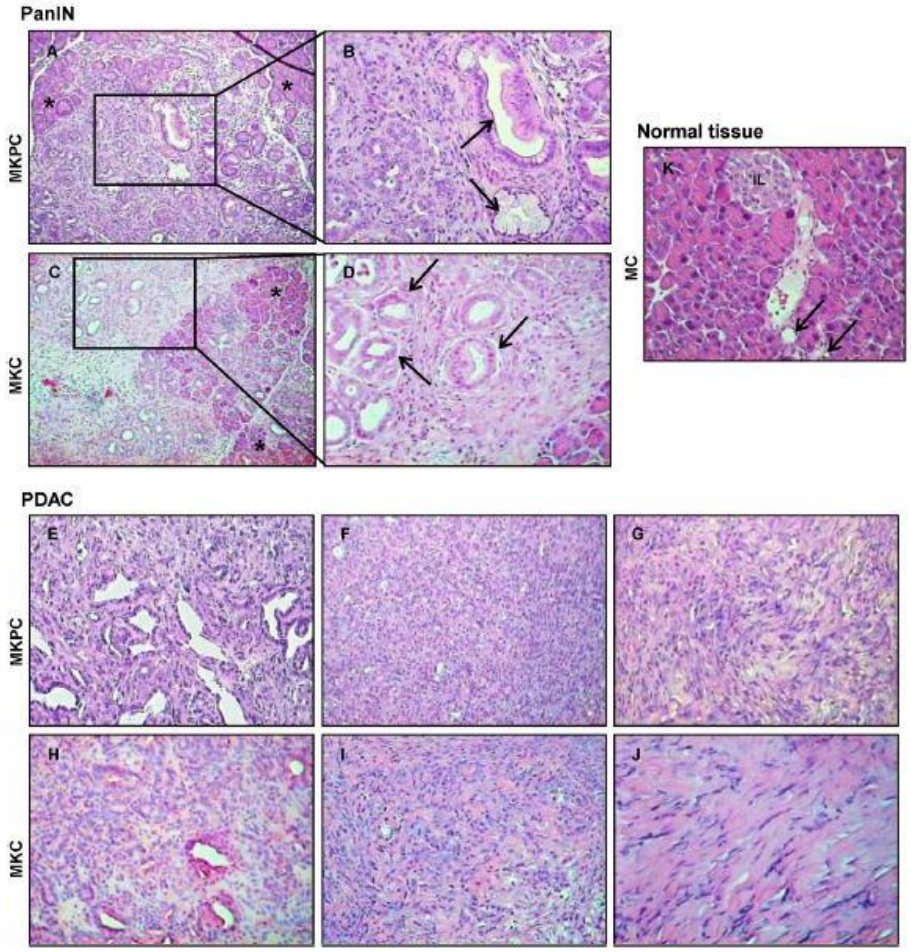

Fig. 2. *Histological appearance of invasive pancreatic ductal adenocarcinoma (PDAC) in FVB based MKPC and MKC mice.* Haematoxylin and eosin (H&E) staining of pancreas sections from 11 week old MKPC and MKC mice. (A and C) PanINs (boxes) at the junction between normal acini (asterisks) and invasive PDAC in MKPC (A) and MKC (C) mice (100×). (B and D) PanINs (arrows) at higher magnification in MKPC (B) and MKC (D) mice (250X). (E–J) Architectural features of invasive PDAC in MKPC (E–G) and MKC (H–J) mice (250×). (E and H) Well-differentiated regions of PDAC showing prominent glandular and acinar architecture in MKPC (E) and MKC (H) mice; (F and I) regions of poorly differentiated PDAC in MKPC (F) and MKC (I) mice; (G and J) tumour with predominant sarcomatoid differentiation (spindle cell type) in MKPC (G) and MKC (J) mice. (K) MC mice pancreas shows normal cuboidal ductal epithelium (arrows), islet of Langherans (IL), and surrounding acinar tissue (250×).

Please cite this article in press as: de Latouliere, L., et al., A bioluminescent mouse model of proliferation to highlight early stages of pancreatic cancer: A suitable tool for preclinical studies. Ann. Anatomy (2015), http://dx.doi.org/10.1016/j.aanat.2015.11.010

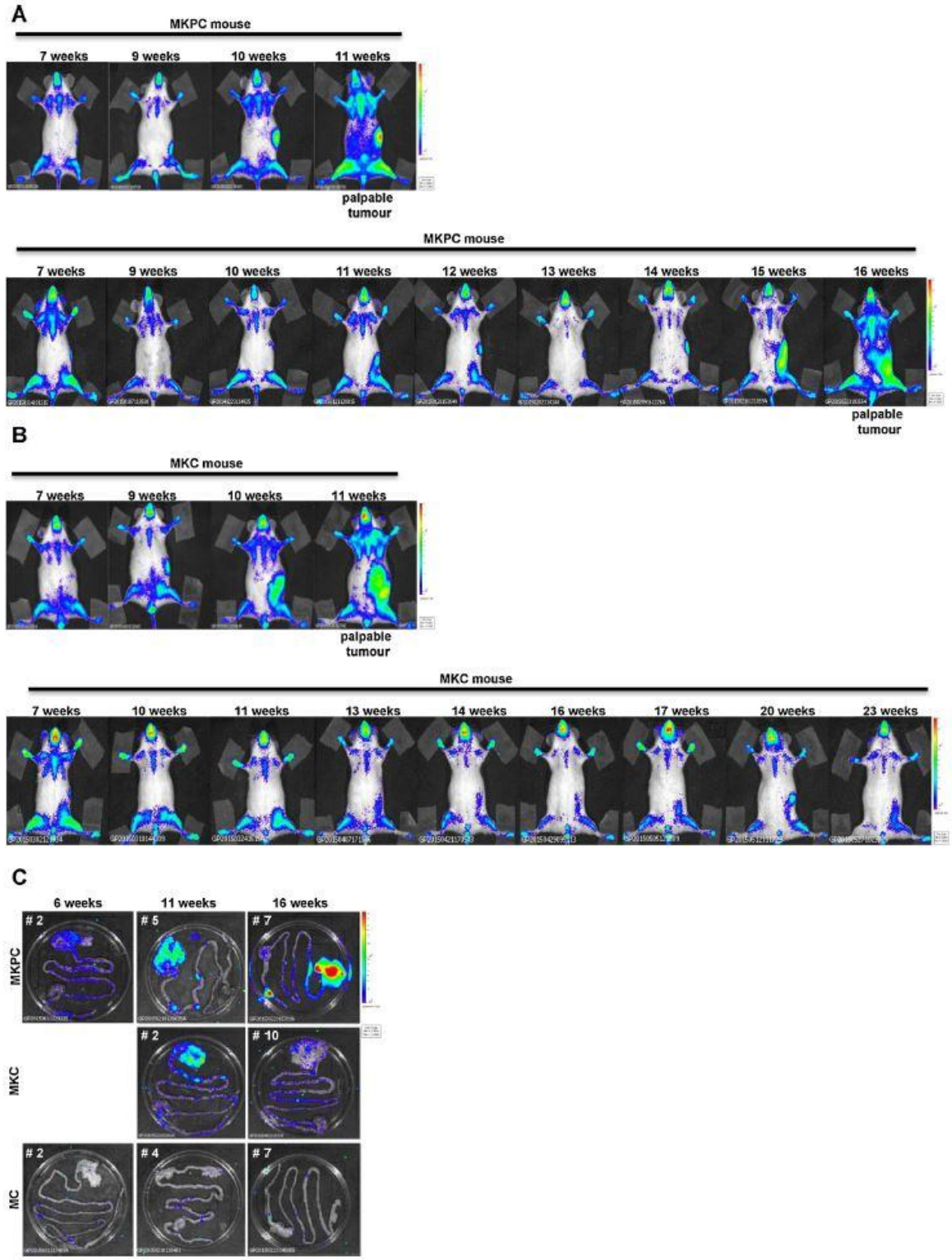

Fig. 3. *Longitudinal monitoring of PDAC associated proliferation by in vivo and ex vivo BLI. In vivo* BLI of two MKPC (A) and two MKC (B) representative mice respectively, at the indicated weeks. The images were collected from 13 MKPC and 17 MKC mice, respectively; two representative animals per group are shown. (A) The two MKPC mice developed tumours at 11 and 16 weeks old, respectively. (B) One of the two MKC mice developed tumours at 11 weeks of age while the other did not develop tumour until 23 weeks. (C) *Ex vivo* BLI of pancreas from MKPC, MKC and MC mice. After the animals were sacrificed, the pancreas were collected at the indicated weeks of age. Images of five animals for each genotype were collected and one representative animal is shown. Both in A and B, light emitted from the animal appears in pseudocolor scaling.

Please cite this article in press as: de Latouliere, L., et al., A bioluminescent mouse model of proliferation to highlight early stages of pancreatic cancer: A suitable tool for preclinical studies. Ann. Anatomy (2015), http://dx.doi.org/10.1016/j.aanat.2015.11.010

Table 2
Histopatology and *ex vivo* BLI signal quantification (p/s/cm²/sr) in MKPC, MKC and MC mice. MKPC = *MITO-Luc;LSL-Kras$^{G12D/+}$;LSL-Trp53$^{R172H/+}$;Pdx-1-Cre*; MKC = *MITO-Luc;LSL-Kras$^{G12D/+}$;Pdx-1-Cre*; MC = *MITO-Luc;Pdx-1-Cre*; PDAC = pancreatic ductal adenocarcinoma.

MKPC	Week old	Histopathology	Avg radiance (p/s/cm²/sr)
1	6	PanINs grade 1-A and 1-B	6.40E + 05
2	6	PDAC, well differentiated	8.64E + 05
3	8	PDAC, well and poorly differentiated regions	9.54E + 06
4	8	PDAC, well differentiated	8.54E + 05
5	11	PDAC, poorly differentiated	5.02E + 06
6	11	PDAC, well differentiated	1.83E + 06
7	16	PDAC, poorly differentiated	3.93E + 07
MKC			
1	11	PanINs grade 1-A and 1-B; rare PanINs grade 2–3	2.08E + 06
2	11	PanINs grade 1-A and 1-B	3.14E + 06
3	11	PDAC, well differentiated	2.24E + 06
4	11	PanINs grade 1-A and 1-B	n.d.
5	11	rare PanINs grade 1-A and 1-B	n.d.
6	11	PanINs grade 1-A and 1-B	n.d.
7	11	rare PanINs grade 1-A	n.d.
8	11	PanINs grade 1-A and 1-B, rare PanINs grade 2–3	n.d.
9	14	PanINs 1-A and 1-B grade	7.67E + 05
10	14	early PDAC, well differentiated	7.19E + 05
11	16	PanINs 1-A and 1-B grade	n.d.
12	17	PanINs grade 1-A and 1-B, rare grade PanINs 2–3	n.d.
MC			
1	6	Normal pancreatic tissue, no PanINs	n.d.
2	8	Normal pancreatic tissue, no PanINs	3.27E + 05
3	8	Normal pancreatic tissue, no PanINs	6.58E + 05
4	11	Normal pancreatic tissue, no PanINs	4.25E + 05
5	11	Normal pancreatic tissue, no PanINs	n.d.
6	11	Normal pancreatic tissue, no PanINs	n.d.
7	16	Normal pancreatic tissue, no PanINs	2.95E + 05

premalignant stages of pancreatic cancer development. For this purpose, MKPC and MKC were subjected to longitudinal *in vivo* imaging sessions starting at 6 weeks of age for several weeks until detection of a palpable tumour. Representative examples of MKPC mice developing tumours at 11 and 16 weeks of age, respectively, are shown in Fig. 3A. Of note, in these mice, a significant induction of abdominal luminescence was already observed one week before the palpable tumour could be detected indicating that imaging proliferation in these mice may allow an early detection of pancreatic cancer progression. In Fig. 3B two examples of MKC mice are shown, one developing tumour at 11 weeks of age (mouse # 355) and the other who did not develop cancer even at 23 weeks of age (mouse # 180). In the first mouse, abdominal bioluminescence was observed one week before the palpable tumour was detected as well as at the week in which the tumour was palpable. In contrast, no induction of abdominal luminescence was observed in the pancreas of the MKC mouse that did not develop cancer (Fig. 3B) and in MC control mice of any age (Supplementary Fig. 1). *In vivo* imaging is carried out in two dimensions; thus the definition of the organ/tissue contributing to the photon emission is limited. To confirm the origin of the photon emissions from MKPC and MKC, the mice were sacrificed when the tumour became palpable and the gastrointestinal apparatus was subjected to *ex vivo* imaging. Examples of this analysis, shown in Fig. 3C, demonstrate that specific spots of BLI signals, although to a different extent, are emitted by the pancreatic mass in both mouse models. Interestingly, at 16 weeks of age, bioluminescence signals from pancreas of MKPC mice were more intense than those from pancreas of MKC mice. Although, in these experiments, we did not reach a statistically significant sample size and further experiments are necessary to confirm this issue, these preliminary results are in agreement with our previous data demonstrating a crosstalk between mutant forms of *p53* protein and NF-Y that sustain an aberrant proliferation in cancer cells (Di Agostino et al., 2006). Moreover, the more intense *ex vivo* BLI signals observed in MKPC *vs* MKC mice were found to be positively associated with the presence of PDAC, which was histologically detected more often in the former transgenic model (Table 2). As expected, the bioluminescence signals are not present in the gastrointestinal apparatus of MC mice.

Altogether, *in vivo* and *ex vivo* analyses demonstrate that MKPC and MKC mouse models are powerful tools to visualize PDAC development in terms of proliferation in the entire living animal in a *spatio*-temporal manner. Most notably, these results also demonstrate that, in these mouse models, it is possible to identify early steps of pancreatic carcinogenesis non-invasively in living animals in which proliferation events take place before tumour appearance. From a pharmacological point of view, this opens the possibility to design therapeutic protocols with a more precise timing than those using the tumour palpability as a starting point, a parameter of low specificity and sensitivity. Moreover, BLI technique is considerable more user-friendly and less expensive than other *in vivo* imaging techniques such as MRI. Finally, from an ethical point of view, application of BLI technique offers interesting additive values, too. Indeed, the analysis is carried out on the same living animal with a series of imaging sessions comfortable for the subject. Most important, this technique allows longitudinal experiments without sacrificing groups of mice at each time point thus reducing the necessary number of animals.

Acknowledgements

We thank Daniela Bona for secretarial assistance, Cinzia Cataldo for technical assistance in histology processing and the Regina Elena Institute animal house (SAFU) for mouse breeding. This work has been partially supported by Italian Association for Cancer Research (AIRC) (IG-2012 n. IG13234) and Cariplo Foundation 2009-2439 to G.P.; Ministero della Sanità-Progetti Ricerca Sanitaria Finalizzata (RF-2013-02354892 to F.N.); Associazione Italiana Ricerca sul Cancro (5× mille no. 12182) and (IG no. 15257) to F.N.; University of Turin-Progetti di Ateneo 2011 (grant

Rethe-ORTO11RKTW) and Progetti Ateneo 2014-Compagnia di San Paolo (PC-METAIMMUNOTHER to F.N. and P.C.); PANTHER to P.C.; Sapienza University of Rome ("Progetto Ateneo 2013") to S.M.; IRE internal projects to G.L.G.

We are indebted to Dr Silvia Bacchetti, McMaster University, Hamilton, Canada for critical reading of the manuscript and for helpful and stimulating discussions.

Appendix A. Supplementary data

Supplementary data associated with this article can be found, in the online version, at http://dx.doi.org/10.1016/j.aanat.2015.11.010.

References

Capello, M., Cappello, P., Linty, F.C., Chiarle, R., Sperduti, I., Novarino, A., Salacone, P., Mandili, G., Naccarati, A., Sacerdote, C., Beghelli, S., Bersani, S., Barbi, S., Bassi, C., Scarpa, A., Nisticò, P., Giovarelli, M., Vineis, P., Milella, M., Novelli, F., 2013. Autoantibodies to Ezrin are an early sign of pancreatic cancer in humans and in genetically engineered mouse models. J. Hematol. Oncol. 6, 67–79.

Cappello, P., Rolla, S., Chiarle, R., Principe, M., Cavallo, F., Perconti, G., Feo, S., Giovarelli, M., Novelli, F., 2013. Vaccination with ENO1 DNA prolongs survival of genetically engineered mice with pancreatic cancer. Gastroenterology 144, 1098–1106.

Cappello, P., Novelli, F., 2013. A self antigen reopens the games in pancreatic cancer. Oncoimmunology 1, e24384.

Di Agostino, S., Strano, S., Emiliozzi, V., Zerbini, V., Mottolese, M., Sacchi, A., Blandino, G., Piaggio, G., 2006. Gain of function of mutant p53: the mutant p53/NF-Y protein complex reveals an aberrant transcriptional mechanism of cell cycle regulation. Cancer Cell 10, 191–202.

Farina, A., Manni, I., Fontemaggi, G., Tiainen, M., Cenciarelli, C., Bellorini, M., Mantovani, R., Sacchi, A., Piaggio, G., 1999. Down-regulation of cyclin B1 gene transcription in terminally differentiated skeletal muscle cells is associated with loss of functional CCAAT-binding NF-Y complex. Oncogene 18, 2818–2827.

Goeman, F., Manni, I., Artuso, S., Ramachandran, B., Toietta, G., Bossi, G., Rando, G., Cencioni, C., Germoni, S., Straino, S., Capogrossi, M., Bacchetti, S., Maggi, A., Sacchi, A., Ciana, P., Piaggio, G., 2012. Molecular imaging of nuclear factor-Y transcriptional activity maps proliferation sites in live animals. Mol. Biol. Cell 23, 1467–1474.

Gurtner, A., Manni, I., Fuschi, P., Mantovani, R., Guadagni, F., Sacchi, A., Piaggio, G., 2003. Requirement for down-regulation of the CCAAT-binding activity of the NF-Y transcription factor during skeletal muscle differentiation. Mol. Biol. Cell 14, 2706–2715.

Gurtner, A., Fuschi, P., Magi, F., Colussi, C., Gaetano, C., Dobbelstein, M., Sacchi, A., Piaggio, G., 2008. NF-Y dependent epigenetic modifications discriminate between proliferating and postmitotic tissue. PLoS ONE 3, e2047.

Gurtner, A., Fuschi, P., Martelli, F., Manni, I., Artuso, S., Simonte, G., Ambrosino, V., Antonini, A., Folgiero, V., Falcioni, R., Sacchi, A., Piaggio, G., 2010. Transcription factor NF-Y induces apoptosis in cells expressing wild-type p53 through E2F1 upregulation and p53 activation. Cancer Res. 70, 9711–9720.

Hidalgo, M., 2012. New insights into pancreatic cancer biology. Ann. Oncol. 23 (Suppl. 10), x135–x138.

Hingorani, S.R., Petricoin, E.F., Maitra, A., Rajapakse, V., King, C., Jacobetz, M.A., Ross, S., Conrads, T.P., Veenstra, T.D., Hitt, B.A., Kawaguchi, Y., Johann, D., Liotta, L.A., Crawford, H.C., Putt, M.E., Jacks, T., Wright, C.V., Hruban, R.H., Lowy, A.M., Tuveson, D.A., 2003. Preinvasive and invasive ductal pancreatic cancer and its early detection in the mouse. Cancer Cell 4, 437–450.

Hingorani, S.R., Wang, L., Multani, A.S., Combs, C., Deramaudt, T.B., Hruban, R.H., Rustgi, A.K., Chang, S., Tuveson, D.A., 2005. Trp53R172H and KrasG12D cooperate to promote chromosomal instability and widelymetastatic pancreatic ductal adenocarcinoma in mice. Cancer Cell 7, 469–483.

Hezel, A.F., Kimmelman, A.C., Stanger, B.Z., Bardeesy, N., Depinho, R.A., 2006. Genetics and biology of pancreatic ductal adenocarcinoma. Genes Dev. 15, 1218–1249.

Manni, I., Mazzaro, G., Gurtner, A., Mantovani, R., Haugwitz, U., Krause, K., Engeland, K., Sacchi, A., Soddu, S., Piaggio, G., 2001. NF-Y mediates the transcriptional inhibition of the cyclin B1, cyclin B2, and cdc25C promoters upon induced G2 arrest. J. Biol. Chem. 276, 5570–5576.

Manni, I., Caretti, G., Artuso, S., Gurtner, A., Emiliozzi, V., Sacchi, A., Mantovani, R., Piaggio, G., 2008. Posttranslational regulation of NF-YA modulates NF-Y transcriptional activity. Mol. Biol. Cell 19, 5203–5213.

Oliva, P., Roncoroni, C., Radaelli, E., Brunialti, E., Rizzi, N., De Maglie, M., Scanziani, E., Piaggio, G., Ciana, P., Komm, B., Maggi, A., 2013. Global profiling of TSEC proliferative potential by the use of a reporter mouse for proliferation. Reprod. Sci. 20, 119–128.

Rizzi, N., Manni, I., Vantaggiato, C., Delledonne, G.A., Gentileschi, M.P., Maggi, A., Piaggio, G., Ciana, P., 2015. In vivo imaging of cell proliferation for a dynamic, whole body, analysis of undesired drug effects. Toxicol. Sci. 145, 296–306.

Sciortino, S., Gurtner, A., Manni, I., Fontemaggi, G., Dey, A., Sacchi, A., Ozato, K., Piaggio, G., 2001. The cyclin B1 gene is actively transcribed during mitosis in HeLa cells. EMBO Rep. 2, 1018–1023.

Signore, A., Mather, S.J., Piaggio, G., Malviya, G., Dierckx, R.A., 2010. Molecular imaging of inflammation/infection: nuclear medicine and optical imaging agents and methods. Chem. Rev. 110, 3112–3145.

Spallotta, F., Cencioni, C., Straino, S., Nanni, S., Rosati, J., Artuso, S., Manni, I., Colussi, C., Piaggio, G., Martelli, F., Valente, S., Mai, A., Capogrossi, M.C., Farsetti, A., Gaetano, C., 2013. A nitric oxide-dependent cross-talk between class I and III histone deacetylases accelerates skin repair. J. Biol. Chem. 288, 11004–11012.

Tuveson, D.A., Hingorani, S.R., 2005. Ductal pancreatic cancer in humans and mice. Cold Spring Harbor Symp. Quant. Biol. 70, 65–72.

Tuveson, D., Hanahan, D., 2011. Translational medicine: cancer lessons from mice to humans. Nature 471, 316–317.